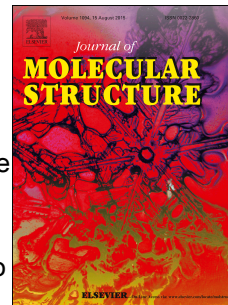


Accepted Manuscript

Molecular modeling of drug-pathophysiological *Mtb* protein targets: Synthesis of some 2-thioxo-1, 3-thiazolidin-4-one derivatives as anti-tubercular agents

Kaveripakkam Mohammed Ali Noorulla, Ayyadurai Jerad Suresh, Vinod Devaraji, Bijo Mathew, Devi Umesh



PII: S0022-2860(17)30930-4

DOI: [10.1016/j.molstruc.2017.07.009](https://doi.org/10.1016/j.molstruc.2017.07.009)

Reference: MOLSTR 24036

To appear in: *Journal of Molecular Structure*

Received Date: 10 March 2017

Revised Date: 5 June 2017

Accepted Date: 7 July 2017

Please cite this article as: K.M. Ali Noorulla, A.J. Suresh, V. Devaraji, B. Mathew, D. Umesh, Molecular modeling of drug-pathophysiological *Mtb* protein targets: Synthesis of some 2-thioxo-1, 3-thiazolidin-4-one derivatives as anti-tubercular agents, *Journal of Molecular Structure* (2017), doi: 10.1016/j.molstruc.2017.07.009.

This is a PDF file of an unedited manuscript that has been accepted for publication. As a service to our customers we are providing this early version of the manuscript. The manuscript will undergo copyediting, typesetting, and review of the resulting proof before it is published in its final form. Please note that during the production process errors may be discovered which could affect the content, and all legal disclaimers that apply to the journal pertain.

Molecular Modeling of Drug-Pathophysiological *Mtb* Protein Targets: Synthesis of some 2-thioxo-1, 3-thiazolidin-4-one derivatives as anti-tubercular agents

Kaveripakkam Mohammed Ali Noorulla^a, Ayyadurai Jerad Suresh^{a*}, Vinod Devaraji^a,
Bijo Mathew^b, Devi Umesh^a

^aDepartment of Pharmaceutical Chemistry, College of Pharmacy, Madras Medical College, Chennai-600003, Tamil Nadu, India.

^bDivision of Drug Design and Medicinal Chemistry Research Lab, Department of Pharmaceutical Chemistry, Ahalia School of Pharmacy, Palakkad-678553, Kerala, India.

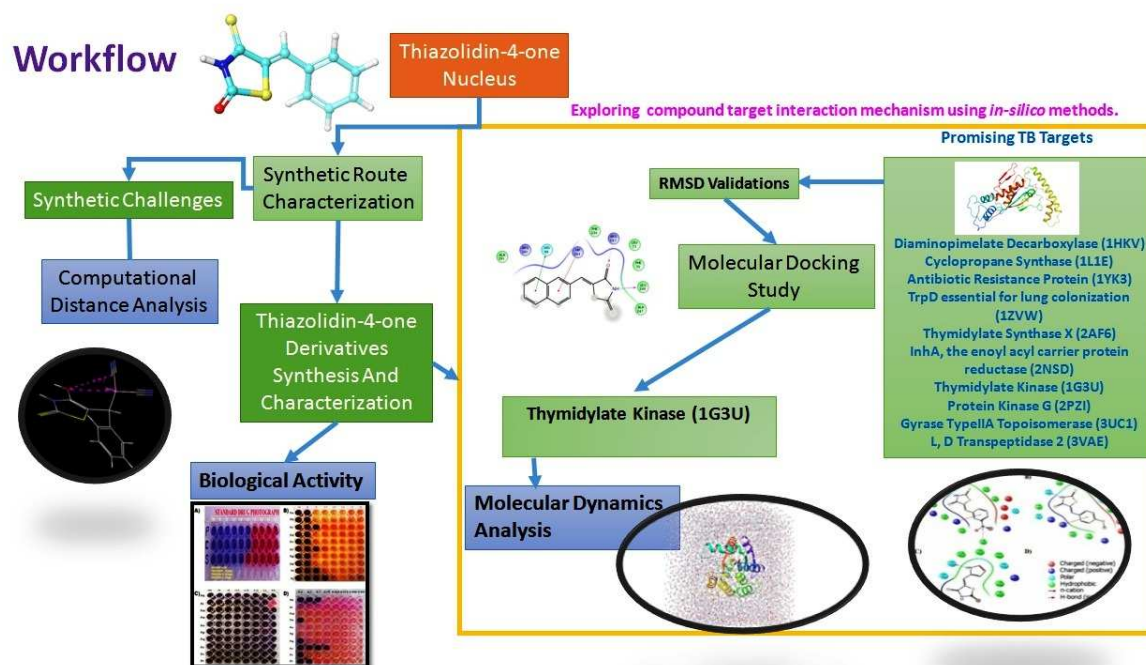
*Corresponding author: Ayyadurai Jerad Suresh
Tel: +919381037921
Email address: ajsuresh2001@yahoo.co.uk

Abstract

Twenty novel 2-thioxo-1, 3-thiazolidin-4-one derivatives (**5a-5t**) were synthesized and evaluated for their antitubercular activity. The structure of the compounds was confirmed by IR, NMR and Mass Spectroscopy methods. In addition, single-crystal X-ray diffraction was performed for compound **5a**. All the synthesized compounds were screened for their *in-vitro* antimycobacterial activity against MTB (H37RV, ATCC No: 27294) by Alamar Blue assay method. Compounds **5r**, **5k**, **5t** displayed most potent *in-vitro* activity with MICs of 0.05, 0.1, 0.2 µg/ml concentrations respectively which are comparatively potent than the standards. Molecular docking and dynamics simulations were performed to find out the plausible mechanism of the titled compounds.

Keywords: *Mycobacterium tuberculosis*, 4-thiazolidinones, Malononitrile, Molecular dynamics.

Graphical Abstract



Highlights

- Twenty 2-thioxo-1, 3-thiazolidin-4-one derivatives were synthesized.
- Exploration of the synthetic route by Computational Distance Analysis.
- *In-vitro* Anti-tubercular activity by Alamar blue assay was performed.
- Ligand Target Interaction mechanism using *in-silico* methods were explored.
- Molecular docking and dynamics calculations were performed.

1. Introduction

Tuberculosis, MTB, or TB is an infectious disease caused by various strains of mycobacteria, usually *Mycobacterium tuberculosis* [1]. It has become an important world-wide public health problem with one-third of the world's population infected by the TB bacillus. Tuberculosis typically attacks the lungs, but can also affect other parts of the body. It is spread through the air when people who have an active TB infection cough, sneeze or otherwise transmit respiratory fluids through the air [2]. According to World Health Organization (WHO), one-third of the world's population is thought to have been infected with *M. tuberculosis* [3] and new infections occur in about 1% of the population each year [4]. In 2007, an estimated 13.7 million chronic cases were active globally [5], while in 2013, an estimated 9 million new cases occurred [6]. In

2013 about 1.3 and 1.5 million associated deaths were reported [6, 7], most of which occurred in the developing countries [8]. People with weak immune systems (those with HIV/AIDS, those receiving immunosuppressive drugs and chemotherapy) are at a greater risk for developing TB disease. There is currently a growing concern about the development and discovery of multidrug which extensively would be drug-resistant tuberculosis (MDR/XDR-TB) with potential to paralyze TB care programs.

Furthermore, no new drugs have been introduced in the last four decades, except the recently introduced fluoroquinolones [9, 10], which testifies to the lack of significant research in this area in the pharmaceutical industry. Hence the development of new drugs, capable of overcoming MDR- and XDR-TB, to efficiently treat this disease is imperative.

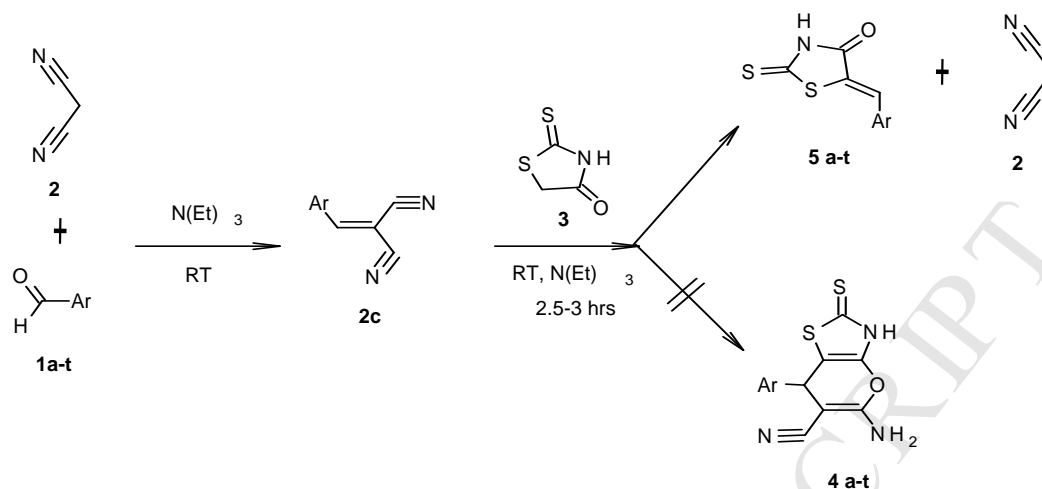
Small ring heterocycles containing nitrogen, sulfur and oxygen have been under investigation for a long time for their medicinal properties. Of these, the 4-thiazolidinones were found to possess various biological activities such as antibacterial, antifungal, diuretic, antihistaminic, anticonvulsant, anticancer, antiviral, anti-HIV, anti-inflammatory and analgesic properties [11-22]. Further, 4-thiazolidinones were found to possess potent antitubercular properties [23-26]. In the view of above facts and in the continuation of our search for new class of anti-tubercular heterocyclic compounds, we report herein synthesis, anti-tubercular activity, *in-silico* ADME properties, molecular docking studies and molecular dynamic studies of some 2-thioxo-1, 3-thiazolidin-4-one derivatives.

2. Results and discussion

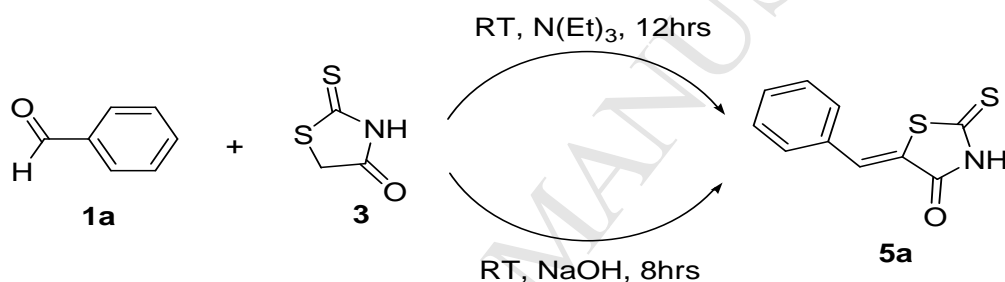
2.1 Chemistry

In our initial endeavor, we have investigated a sequential three component reaction of benzaldehyde **1a**, malononitrile **2** and 2-thioxo-1, 3-thiazolidin-4-one **3** in ethanol and in presence of triethylamine base under room temperature and stirring to afford functionalized pyranothiazole derivative 5-amino-7-phenyl-2-thioxo-3, 7-dihydro-2H-pyrano [2, 3-d] [1, 3] thiazole-6-carbonitrile **4a**. However, the reaction did not give the expected pyranothiazole derivative **4a** and instead, only one compound by simple filtration was isolated in good yield and identified as 5-benzylidene-2-thioxo-1, 3-thiazolidin-4-one **5a** (Scheme 1).

The structure of **5a** was further verified by TLC, m.p. and mixed m.p after independent synthesis via direct condensation of benzaldehyde **1a** with 2-thioxo-1, 3-thiazolidin-4-one **3** in the presence of bases like triethylamine and NaOH. However, the independent synthetic method suffers from longer reaction times and requires aqueous workup procedures for the isolation of compound (Scheme 2).



Scheme 1: Synthesis of 2-thioxo-1,3-thiazolidin-4-one derivatives.



Scheme 2: Synthesis of compound 5a via direct condensation.

A plausible mechanism was proposed for the formation of compound **5a** and for the non-formation of the compound **4a** (**Scheme 3**). Initially, the reaction proceeded through the generation of malonyl adduct **2c** via the Knoevenagel condensation of benzaldehyde **1a** and malononitrile **2** in the presence of triethylamine base. The intermediate **2c** can be isolated and its formation was identified by TLC. Compound **2c** a key intermediate undergoes Michael addition with **3a** to give **3c**, which upon enolization gave **3d**. The enol group and cyano group of the intermediate **3d** was expected to undergo nucleophilic addition in order to facilitate an intramolecular *6-exo-dig* cyclization process followed by a rearrangement via proton transfer to yield compound **4a**. Such an intramolecular cyclization process in **3d** was not occurred to generate compound **4a** instead elimination of malononitrile took place leading to the formation of compound **5a** and the structure was confirmed by IR, NMR and Mass Spectroscopy and also by X-Ray Crystallography. The non-formation of the compound **4a** is likely the result of the non-optimal distance between the reactive centres (enol group and cyano group) of **3d** for nucleophilic attack due to geometrical constraints (**Figure 1**).

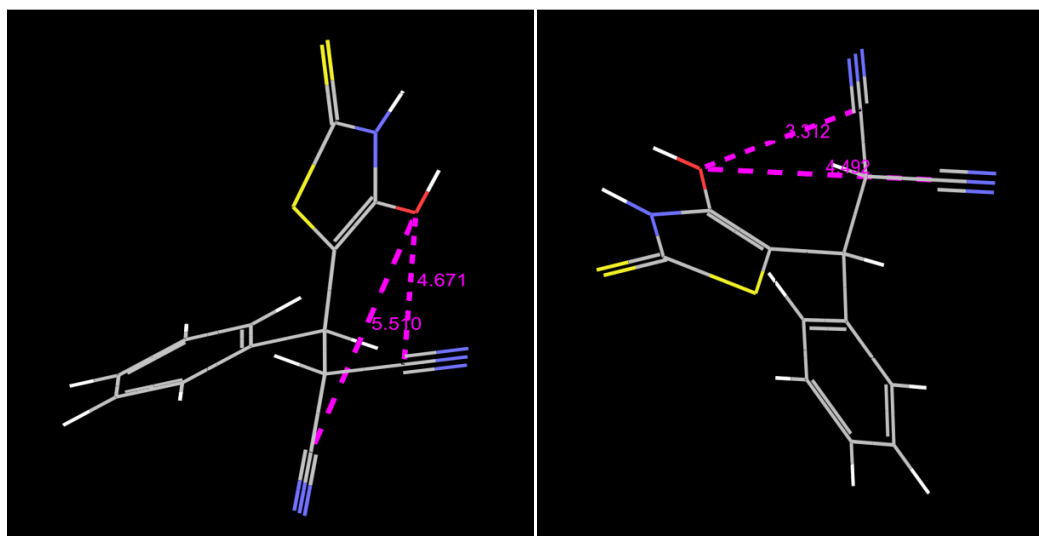
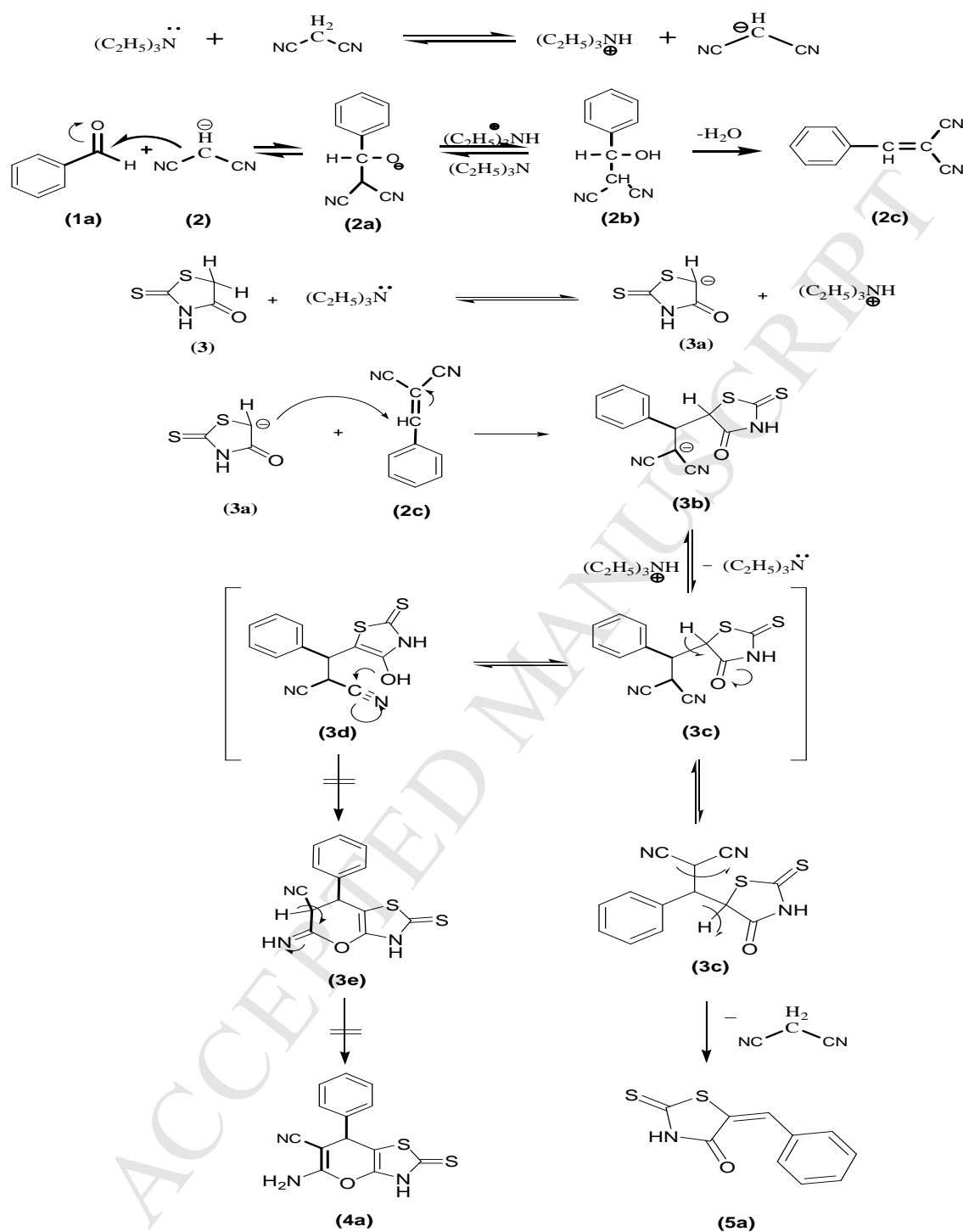


Figure 1:Distance between the reactive centres (enol and cyano group) of intermediate **3d**.

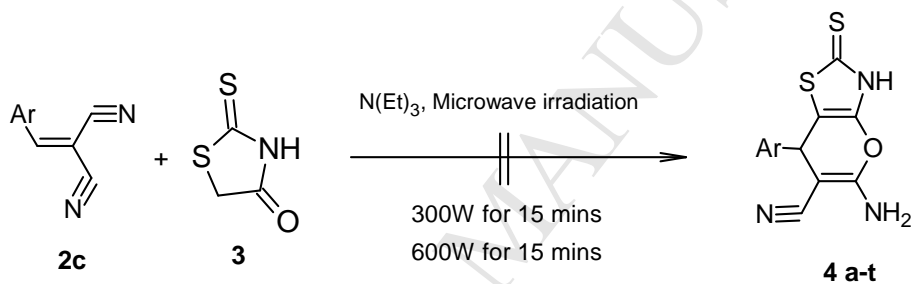


Scheme 3: Plausible mechanism for the formation of compound **5a** and non-formation of compound **4a**.

In the view of intramolecular *6-exo-dig* cyclization process to take place, the above reaction was also attempted in different solvent systems like methanol, toluene and acetonitrile and in

presence of different catalysts like InCl_3 , sodium hydroxide and pyridine under reflux conditions. In all cases, no evolution of compound **4a** was detected. Compound **5a** was detected by TLC and isolated by simple filtration.

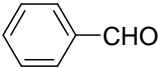
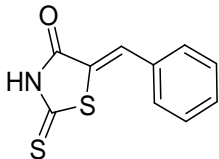
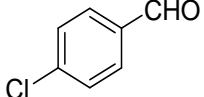
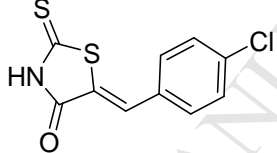
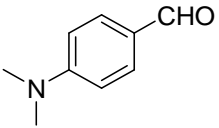
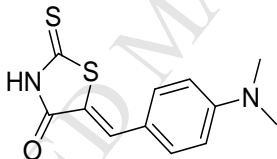
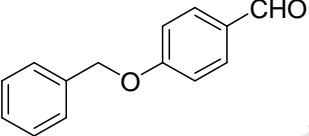
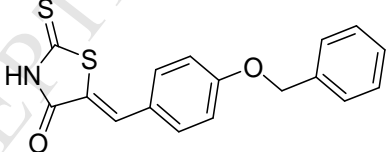
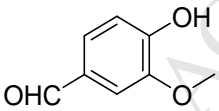
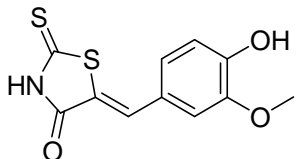
An attempt of reaction under microwave radiation was used to induce intramolecular cyclization on intermediate **3d**. It was expected that microwave would assist the interconversion of conformers through an efficient bond rotation to generate the pyran ring through a favoured 6-*exo-dig* cyclization process. The success of this reaction was expected to depend on the formation of the appropriate conformational isomer. The reaction was carried out using synthetic microwave equipment between the isolated malonyl adduct **2c** and 2-thioxo-1, 3-thiazolidin-4-one **3**, in the presence of catalytic amount of triethylamine in ethanol. The reaction mixture was exposed to microwave at 300W intermittently at 1 min intervals for 15 mins and then at 600W for 15 mins. In both cases, there was no evidence of the intramolecular cyclization for the formation of compound **4a** (Scheme 4).

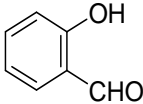
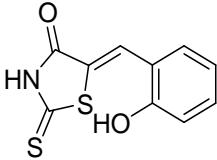
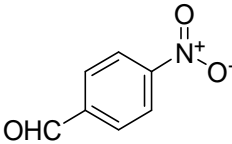
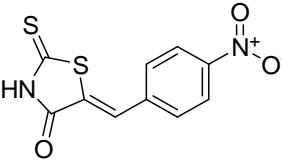
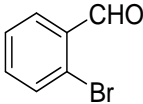
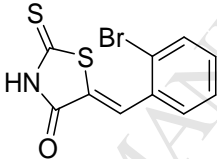
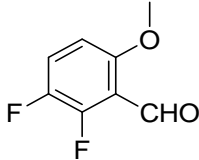
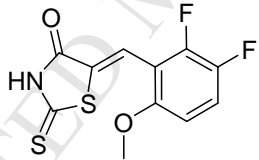
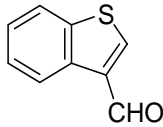
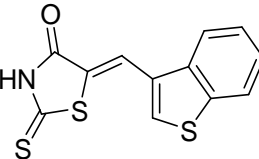
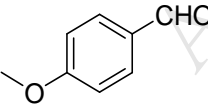
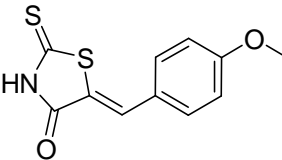


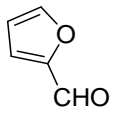
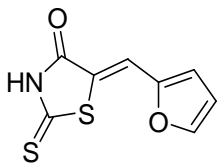
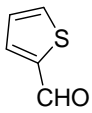
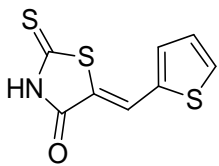
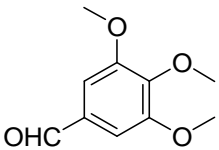
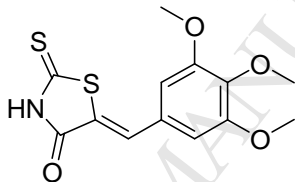
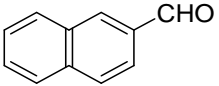
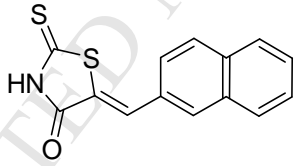
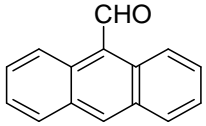
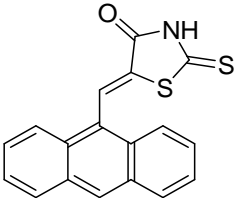
Scheme 4: Reaction of malonyl adduct **2c** and 2-thioxo-1, 3-thiazolidin-4-one **3**.

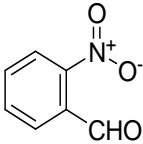
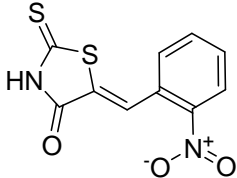
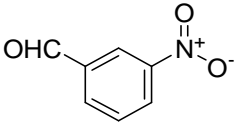
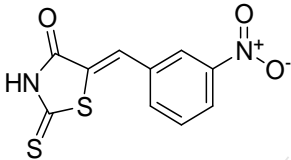
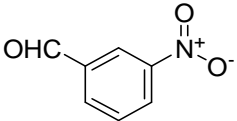
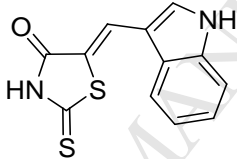
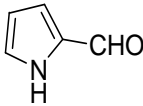
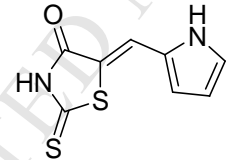
The attempt to synthesize compound **4a** through a favoured intramolecular cyclization process was unsuccessful leading us to conclude that the *in situ* formed intermediate **3d** would be a more stable conformer which averts from cyclization process. Hence understanding the scope and limitations of the reaction, further attention was made in the synthesis of 2-thioxo-1, 3-thiazolidin-4-one derivatives **5 a-t** with various substituted aldehyde derivatives. Under the above reaction conditions, the reaction proceeded smoothly with various aldehydes, including those containing electron withdrawing and electron releasing groups to provide 2-thioxo-1, 3-thiazolidin-4-one derivatives **5 a-t** in good yields (84–95%). The results are given in **Table 1**.

Table: 1 Synthesis of 2-thioxo-1, 3-thiazolidin-4-one derivatives **5 a-t**

Entry	Product	Ar-CHO	Structures	IUPAC name	Yield (%)
1	5a			“(Z)-5-benzylidene-2-thioxothiazolidin-4-one”	92
2	5b			“(Z)-5-(4-chlorobenzylidene)-2-thioxothiazolidin-4-one”	86
3	5c			“(Z)-5-(4-(dimethylamino)benzylidene)-2-thioxothiazolidin-4-one”	95
4	5d			“(Z)-5-(4-(benzyloxy)benzylidene)-2-thioxothiazolidin-4-one”	89
5	5e			“(Z)-5-(4-hydroxy-3-methoxybenzylidene)-2-thioxothiazolidin-4-one”	90

6	5f			“(Z)-5-(2-hydroxybenzylidene)-2-thioxothiazolidin-4-one”	88
7	5g			“(Z)-5-(4-nitrobenzylidene)-2-thioxothiazolidin-4-one”	85
8	5h			“(Z)-5-(2-bromobenzylidene)-2-thioxothiazolidin-4-one”	92
9	5i			“(Z)-5-(2,3-difluoro-6-methoxybenzylidene)-2-thioxothiazolidin-4-one”	93
10	5j			“(Z)-5-((benzo[b]thiophen-3-yl)methylene)-2-thioxothiazolidin-4-one”	88
11	5k			“(Z)-5-(4-methoxybenzylidene)-2-thioxothiazolidin-4-one”	87

12	5l			“(Z)-5-((furan-2-yl)methylene)-2-thioxothiazolidin-4-one”	85
13	5m			“(Z)-5-((thiophen-2-yl)methylene)-2-thioxothiazolidin-4-one”	92
14	5n			“(Z)-5-(3,4,5-trimethoxybenzylidene)-2-thioxothiazolidin-4-one”	84
15	5o			“(Z)-5-((naphthalen-2-yl)methylene)-2-thioxothiazolidin-4-one”	89
16	5p			“(Z)-5-((anthracen-9-yl)methylene)-2-thioxothiazolidin-4-one”	90

17	5q			“(Z)-5-(2-nitrobenzylidene)-2-thioxothiazolidin-4-one”	85
18	5r			“(Z)-5-(3-nitrobenzylidene)-2-thioxothiazolidin-4-one”	94
19	5s			“(Z)-5-((1H-indol-3-yl)methylene)-2-thioxothiazolidin-4-one”	86
20	5t			“(Z)-5-((1H-pyrrol-2-yl)methylene)-2-thioxothiazolidin-4-one”	88

The structures of the 2-thioxo-1, 3-thiazolidin-4-one derivatives **5 a-t** were established from IR, ¹H NMR, ¹³C NMR and Mass spectroscopic data. IR spectra in general showed =CH peak in the regions of 3109-2839 cm⁻¹. In the 1H NMR spectra the signals of the respective protons of the synthesized compounds were confirmed based on their chemical shifts, multiplicities and coupling constants. These spectra showed a singlet at around δ 7.60 ppm, which corresponds to the -CH=. The ¹³C NMR and elemental analysis were in accordance to the synthesized structure. Elemental analysis results were within ±0.4% of the theoretical values. The appearance of their respective molecular ion peaks (M⁺) in the mass spectroscopy also confirms the formation of the compounds. The relative stereochemistry of the product **5a** was established through single-crystal X-ray analysis (**Figure 2**).

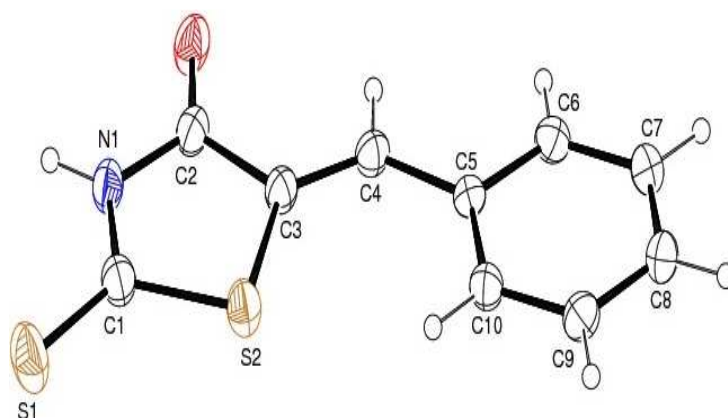


Figure 2: ORTEP diagram of compound **5a**

2.2 Pharmacology

All the synthesized compounds were screened for their *in-vitro* antimycobacterial activity against MTB (H37RV, ATCC No: 27294) by Alamar Blue assay (MABA) method [27]. Pyrazinamide, Ciprofloxacin and streptomycin were used as reference drugs. The results were represented as minimum inhibitory concentration (MIC) (**Figure 3**) and are presented in **Table 2**.

When screened against MTB the synthesized thiazolidinone derivatives **5 a-t** showed moderate to potent *in vitro* activity against MTB with MIC range **0.05-50 µg/ml**. Compounds **5r**, **5k**, **5t** displayed most potent *in-vitro* activity with MICs **0.05**, **0.1**, **0.2 µg/ml** concentrations respectively. Further, compounds **5n**, **5q**, **5s**, **5m**, **5o**, **5p**, **5l** showed potent *in-vitro* activity with MIC range **0.4 to 1.6 µg/ml** concentrations, while other compounds shown moderate to good activity.

The influence of the different chemical groups on the observed antimycobacterial activity against MTB deserves comment. Incorporation of nitro group at 3rd position of the phenyl ring (**Compound 5r**) led to show potent inhibition of *M tuberculosis* at 0.05 µg/ml concentration, while nitro position at 2nd and 4th position of the phenyl ring (**Compound 5q and 5g**) led to reduction of the activity 8 and 100 times respectively. Introduction of mono-methoxy group at 4th position of the phenyl ring (**Compound 5k**) also exhibited potent inhibition at 0.1 µg/ml concentration, while tri-methoxy group at 3rd, 4th and 5th positions (**Compound 5n**) reduced the activity 8 times. The phenyl substitution (**Compound 5a**) showed moderate activity at 50 µg/ml concentration whereas there is a tenfold increase in activity in case of naphthalene and anthracene aromatic hydrocarbon substitution (**Compound 5o and 5p**). Conversely five membered heterocyclic rings in the place of six membered rings (**Compound 5j, 5l, 5m, 5s and 5t**) increased the activity remarkably. Furthermore halogen substitution of the phenyl ring (**Compound 5b, 5h and 5i**) showed moderate activity.

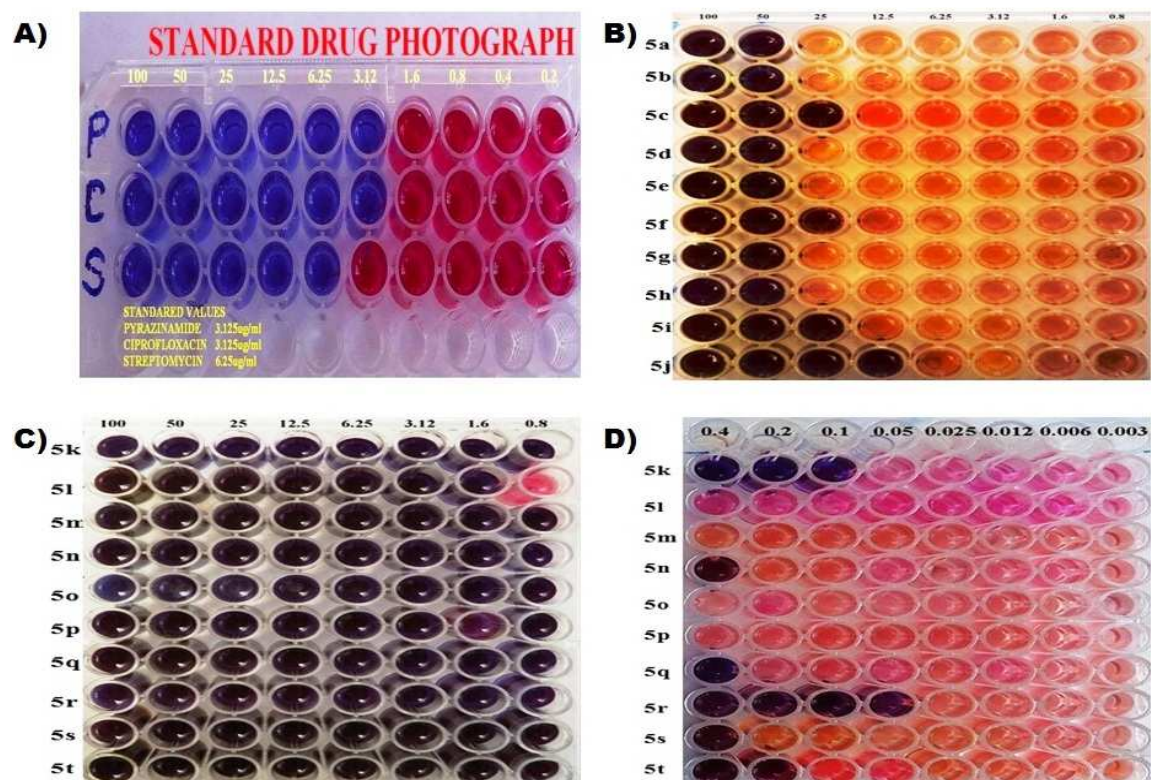


Figure 3: A) Antimycobacterial activity of standard drugs Pyrazinamide, Ciprofloxacin and Streptomycin. B) Antimycobacterial activity of compounds **5 a-j** tested at **100-0.8 µg/ml** concentrations. C) Antimycobacterial activity of compounds **5 k-t** tested at **100-0.8 µg/ml** concentrations. D) Antimycobacterial activity of compounds **5 k-t** tested at **0.4-0.003 µg/ml** concentrations.

Table 2: Antimycobacterial activity of *2-thioxo-1, 3-thiazolidin-4-one* derivatives

Entry	Product	MIC (µg/ml)	Ranking ^a
1.	5a	50	20
2.	5b	50	19
3.	5c	12.5	13
4.	5d	50	18
5.	5e	50	15
6.	5f	12.5	14
7.	5g	50	17

8.	5h	50	16
9.	5i	25	12
10.	5j	12.5	11
11.	5k	0.1	2
12.	5l	1.6	10
13.	5m	0.8	7
14.	5n	0.4	6
15.	5o	0.8	8
16.	5p	0.8	9
17.	5q	0.4	4
18.	5r	0.05	1
19.	5s	0.4	5
20.	5t	0.2	3
21.	Pyrazinamide	3.12	-
22.	Ciprofloxacin	3.12	-
23.	Streptomycin	6.25	-

^a - ranking of synthetic compounds based on the *in-vitro* antitubercular activity data

2.3 Computational Chemistry

Computational chemistry approach is the most dynamic technology, which had gained lot of prominence in modern drug discovery [28]. So we were inquisitive in understanding and knowing the features in our synthesized compounds that are accountable for inhibitory activity.

2.3.1 In-silico ADME Properties

The QikProp (Schrodinger[®]) is the prediction tool used to obtain the pharmacokinetics and pharmacodynamics of the analogues by assessing the drug like properties. The structures of the synthesized compounds were built using Maestro (Schrodinger[®]) build panel. All the ligands were prepared by using Ligprep (Schrodinger[®]) which uses OPLS_2005 (Optimized Potential for Liquid Simulations) force field and gave the corresponding low energy 3D conformers of the

ligands. The low energy 3D conformers of the ligands were checked for their ADME properties using QikProp (Schrodinger[®]).

QikProp (Schrodinger[®]) prediction gave information about descriptors like molecular weight (mol_MW), octanol/water partition coefficient (QPlogPo/w), brain/blood partition coefficient (QPlogBB), % human oral absorption (PercentHumanOralAbsorption), human serum albumin binding (QPlogKhsa), IC50 for HERG K⁺ Channel blockage (QPlogHERG), Lipinski's rule of five violations (Rule ofFive). All the compounds were found to be within the range and recommended values for 95% of known drugs. The results are given in **Table 3**.

Table 3: *In-silico* ADME properties of the synthesized compounds

Ligands	MW	QPlog Po/w	QPlog HERG	QPlog BB	QPlog Khsa	Percent HumanOral Absorption	Rule ofFive
5a	221.29	2.28	-4.51	-0.06	-0.19	100	0
5b	255.74	2.91	-4.47	0.10	-0.08	100	0
5c	264.36	2.72	-4.61	-0.19	-0.03	100	0
5d	327.42	4.38	-6.34	-0.37	0.41	100	0
5e	267.32	1.98	-4.43	-0.53	-0.31	89.84	0
5f	237.29	1.77	-4.39	-0.52	-0.34	86.94	0
5g	266.29	1.82	-4.48	-1.01	-0.22	78.54	0
5h	300.19	2.91	-4.40	0.08	-0.07	100	0
5i	287.30	2.78	-4.35	0.01	-0.09	100	0
5j	277.37	3.29	-4.74	0.04	0.08	100	0
5k	251.32	2.54	-4.44	-0.14	-0.17	100	0
5l	211.25	1.86	-4.20	-0.04	-0.42	95.25	0
5m	227.31	2.41	-4.17	0.04	-0.27	100	0
5n	311.37	2.75	-4.25	-0.29	-0.15	100	0
5o	271.35	3.38	-5.23	-0.10	0.17	100	0
5p	321.41	4.38	-5.31	0.09	0.58	100	0
5q	266.29	1.90	-4.43	-0.89	-0.23	80.97	0
5r	266.29	1.82	-4.48	-1.01	-0.22	78.55	0
5s	260.33	2.60	-4.79	-0.33	-0.05	94.77	0
5t	210.27	1.72	-4.09	-0.25	-0.38	90.29	0
Range*	130-725	-2 to 6.5	<-5	-3.0 to 1.2	-1.5 to 1.5	<25 is poor, >80 is high	Maximum upto 4

* - For 95% known drugs

2.3.2 Molecular docking

2.3.2.1 Pose Docking RMSD (Root mean Square deviation):

In order to understand the accuracy of the programs we had carried out docking pose RMSD calculation (Table 4) of co-crystal proteins, where the crystal compound is re-docked using Glide (citation) software and checked for atom to atom with the co-crystal pose. The predictive capability of software is confirmed if the deviation is less. We had done considered all proteins which had co-crystal organic molecules using XP docking mode with all default settings provided by the Glide software. We found that most of the proteins gave good pose reproducibility with crystal interaction retained in all, except 1YK3 as BOD. High flexibility in case of 1YK3/BOD could be the reason for the deviation. Pose reproducibility of protein pdb: 2PZI with ligand id AXX is shown in **Figure 4**.

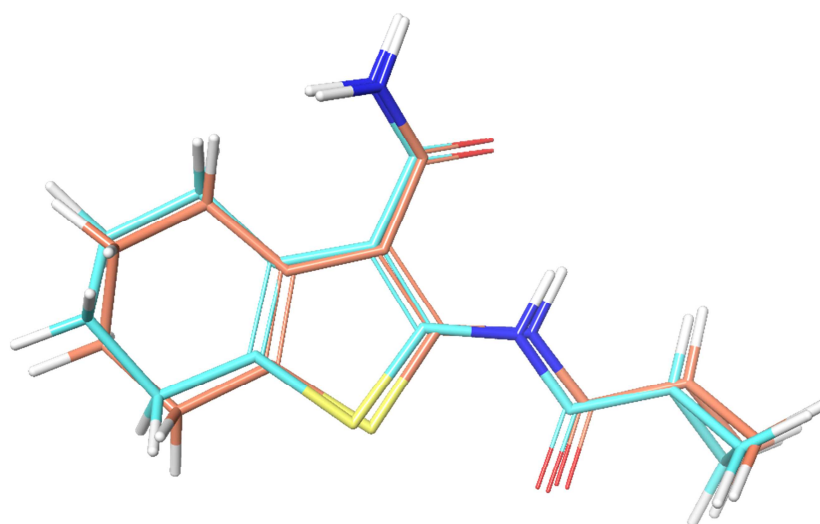


Figure 4: Pose reproducibility of protein pdb: 2PZI with ligand id AXX in thin tube form where light brown is crystal pose and light blue is docked pose.

Table 4: RMSD values of co-crystal proteins

Sl.No	PDB_ID	Ligand ID	Pose RMSD
1	1HKV	PLP	1.43
2	1L1E	SAH	1.23
3	1YK3	BOD	3.45
4	1ZVW	PRP	1.98
5	2AF6	BRU	1.8
6	2NSD	4PI	2.2
7	1G3U	TMP	0.76
8	2PZI	AXX	0.79
9	3UC1	APO	No ligand
10	3VAE	APO (PEG)	No ligand

APO (No crystal Ligand)

In order to understand the nature of interactions and to explain the plausible mechanism of the synthesized compounds for *in-vitro* antitubercular activity, we carried out molecular docking between all the ligands and the active sites of ten pathophysiological tubercular target enzymes. The target enzymes were selected from the target identification pipeline for *Mycobacterium tuberculosis*, which comprises a total of 451 high-confidence targets [29]. The ten high-confidence targets with their PDB ids were selected based on their structural similarity with the synthesized compounds, good X-ray resolution and without structural issues or breaks and are as follows, Diaminopimelate Decarboxylase [30] (PDB id – 1HKV), Cyclopropane Synthase [31] (PDB id – 1L1E), Antibiotic Resistance Protein [32] (PDB id – 1YK3), TrpD essential for lung colonization [33] (PDB id – 1ZVW), Thymidylate Synthase X [34] (PDB id – 2AF6), InhA, the enoyl acyl carrier protein reductase [35] (PDB id – 2NSD), Thymidylate Kinase [36] (PDB id – 1G3U), Protein Kinase G [37] (PDB id – 2PZI), GyraseTypeIIA Topoisomerase [38] (PDB id – 3UC1), L, D Transpeptidase 2 [39] (PDB id – 3VAE). All the targets were retrieved from Protein Data Bank (PDB) and the molecular docking studies were performed using Glide (Schrodinger®) model (Extra Precision XP) of the default parameter settings and the docking scores were summarized in **Table 5**. The overall glide docking scores ranges from -10.62 to -2.00 for all the ligands on all the target enzymes.

Table 5: Glide docking scores of 2-thioxo-1, 3-thiazolidin-4-one analogs (**5a-t**)

Ligands	Glide docking scores in kcal/mol									
	1HKV	1L1E	1YK3	1ZVW	2AF6	2NSD	1G3U	2PZI	3UCI	3VAE
5a	-2.0	-7.0	-5.3	-3.8	-4.2	-8.3	-7.1	-7.1	-2.9	-4.1
5b	-2.0	-6.0	-6.1	-5.2	-4.0	-9.1	-6.3	-6.8	-4.7	-4.3
5c	-1.8	-6.3	-4.6	-5.2	-4.4	-8.7	-3.8	-6.8	-2.6	-4.4
5d	-2.3	-8.8	-7.9	-5.9	-5.4	-10.6	-5.2	-6.4	-4.5	-5.2
5e	-4.1	-6.7	-5.5	-5.3	-4.6	-8.8	-5.8	-6.9	-4.6	-5.5
5f	-2.9	-7.5	-5.2	-4.9	-3.4	-8.1	-3.4	-8.4	-5.3	-5.0
5g	-1.5	-5.6	-5.7	-5.0	-4.0	-8.1	-6.6	-5.7	-3.7	-4.2
5h	-2.0	-5.3	-5.4	-4.3	-4.0	-8.9	-2.8	-5.9	-3.3	-4.3
5i	-2.0	-7.2	-5.2	-4.5	-3.7	-8.7	-2.5	-5.5	-3.5	-5.8
5j	-1.8	-6.2	-5.4	-4.7	-3.3	-9.5	-3.5	-7.5	-4.2	-4.4
5k	-1.4	-5.7	-5.2	-4.8	-3.8	-8.4	-7.6	-6.8	-3.2	-3.2
5l	-3.2	-4.4	-4.7	-3.5	-3.7	-7.2	-7.3	-7.3	-3.9	-5.4
5m	-2.8	-6.4	-4.9	-3.8	-3.6	-7.2	-6.8	-6.9	-4.0	-3.2
5n	-2.6	-6.4	-5.2	-4.6	-4.8	-8.7	-4.5	-5.2	-3.6	-4.7
5o	-3.0	-6.4	-5.2	-4.8	-3.4	-10.3	-5.3	-7.7	-3.6	-4.1
5p	-2.0	-5.9	-6.6	-5.3	-3.8	-9.9	-3.4	-8.9	-3.9	-6.3
5q	-2.3	-4.8	-4.8	-4.3	-3.7	-7.9	-4.3	-5.9	-4.3	-6.3
5r	-1.8	-7.1	-4.7	-3.8	-3.7	-8.3	-6.9	-5.2	-4.5	-4.5
5s	-0.6	-8.3	-4.3	-5.6	-4.4	-8.7	-5.3	-6.9	-5.4	-5.0
5t	-2.7	-6.0	-4.8	-3.8	-4.0	-5.8	-7.4	-6.9	-4.2	-5.1

As per the docking results, all the ligands showed better interactions with the active sites of target enzymes. On comparing the docking results with *in-vitro* antitubercular activity results, top-ranked compounds of *in-vitro* antitubercular activity shows deviation from docking

pose/score rankings in all the studied target enzymes. In order to rationalize the correlation between the *in-vitro* antitubercular activity and docking results a cross observational analysis was performed. The top-ranked three compounds (**5r**, **5k** and **5t**) of *in-vitro* antitubercular activity were cross observed with their docking ranks on all the studied target enzymes for their deviations in ranks. The results are given in **Table 6**. Based upon the results, the docking pose ranking of all the three compounds (**5r**, **5k** and **5t**) showed marginal deviation in thymidylate kinase (PDB id – 1G3U) target enzyme at 5th, 1st and 2nd ranks respectively when compared with docking pose rankings of other target enzymes that were studied. Additionally top three ranked *in-vitro* antitubercular compounds lie within top five positions in thymidylate kinase (PDB id – 1G3U) target enzyme. Thus the study warrants the elimination of false negatives and rationalizes that the enzyme **thymidylate kinase** would be the plausible target for the tested compounds for their *in-vitro* antitubercular activity.

Table 6: Cross observational analysis of top three ranked compounds with docking ranks

Target Enzymes (PDB id)	Ranking positions based on docking scores		
	5r ^a	5k ^a	5t ^a
Diaminopimelate Decarboxylase (1HKV)	17	19	6
Cyclopropane Synthase (1L1E)	5	16	13
Antibiotic Resistance Protein (1YK3)	17	10	18
TrpD essential for lung colonization (1ZVW)	16	10	18
Thymidylate Synthase X (2AF6)	16	12	8
InhA, the enoyl acyl carrier protein reductase (2NSD)	13	12	20
Thymidylate Kinase (1G3U)	5	1	2
Protein Kinase G (2PZI)	20	12	9
GyraseTypeIIA Topoisomerase (3UC1)	7	18	10
L, D Transpeptidase 2 (3VAE)	18	20	7

^a - top three ranked compounds (**5r-1st**, **5k-2nd** and **5t-3rd**) in *in-vitro* antitubercular activity.

The docked pose of the synthesized compound **5d** at the active site of thymidylate kinase is shown in **Figure 5**. The major interactions by the ligands with thymidylate kinase can be categorized as hydrogen bonding, hydrophobic, electrostatic interactions, π - π -stacking and π -

cation-stacking, which are critical for stabilizing the inhibitors inside the binding pocket of the receptor. The important interactions are shown in **Table 7**. The amino acid Asn100 displays strong hydrogen bond interaction with the inhibitors. Arg74 and Tyr39 participate in hydrogen bond interaction in only one inhibitor each, along with Asn100. Other amino acids like Asp163, Arg95, Lys13 and Gly59 also contribute to the hydrogen bonding in some inhibitors. The inhibitors had successfully influenced hydrophobic effect with Tyr39, Tyr103, Tyr165, Pro37, Phe70 and Leu52. Other amino acids like Ala67, Ala35, Ala49, Met66, Val63 and Phe36 also contribute to the hydrophobic interactions. Electrostatic interactions are predominant in inhibitors having interactions with amino acids like Arg74, Arg95, Arg160, Glu166, Asp9 and Asp163. Other weak interactions like π -cation-stacking and π - π -stacking are witnessed in most of the inhibitors with their aromatic group positioned near Arg95, Tyr103 and Phe70. The three top ranked compounds with their ligand interactions are shown in **Figure 6**.

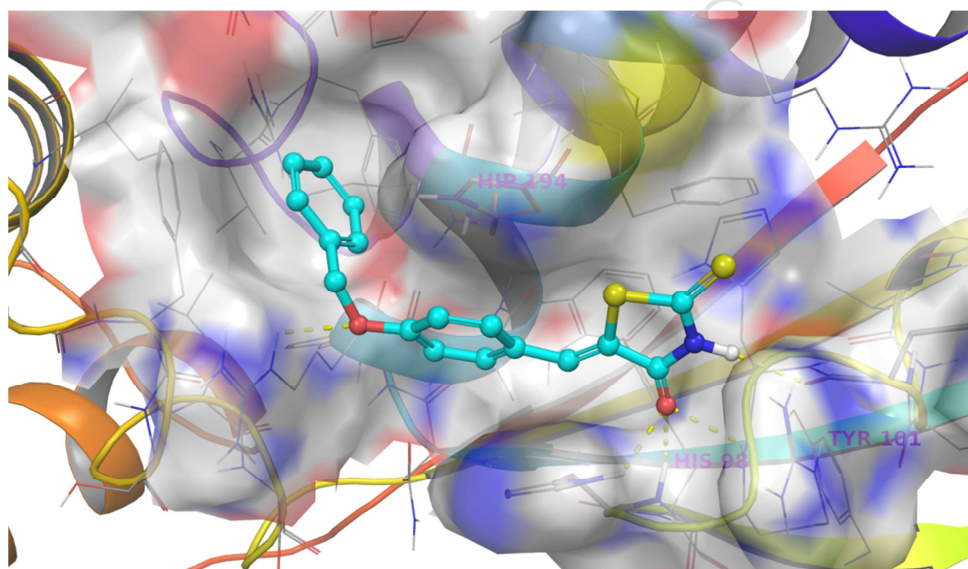


Figure 5: The docked pose of the synthesized compound **5d** at the active site of thymidylate kinase

Table 7: Residue interaction pattern for the synthesized compounds against thymidylate kinase

Ligands	Important Interactions of Ligands with amino acids of binding site of thymidylate kinase (1G3U)				
	Hydrogen Bonding	Hydrophobic	Positive Ionizable	Negative Ionizable	Polar
5a	Asn100	Tyr103, Phe70, Pro37, Tyr39, Leu52, Ala67, Tyr165	Arg74, Arg95	Glu166, Asp9, Asp163	Ser104, Asn100, Ser99,

					Gln172
5b	Asn100, π - cation- stacking- Arg95	Phe36, Phe70, Pro37, Tyr39, Leu52, Tyr103, Tyr165, Ala67	Asp9, Asp163, Glu166	Arg74, Arg95	Ser99, Ser104, Asn100
5c	-	Phe70, Tyr39, Pro37, Leu52, Tyr103, Tyr165, π - π -stacking-Tyr103	Asp9, Asp163, Glu166	Arg74, Lys13, Arg160, Arg153, Arg95	Ser99, Asn100
5d	Gly159	Tyr103, Pro37, Ala49, Leu52, Tyr39, Ala161, Phe70, Tyr165, π - π - stacking-Phe70	Asp9, Asp163, Glu166	Arg95, Arg160	Ser99, Asn100
5e	Asn100, Arg74	Phe36, Tyr96, Pro37, Tyr39, Leu52, Tyr165, Phe70, Tyr103, π - π - stacking-Phe70	Asp9, Asp163, Glu166	Arg74, Arg95, Arg160	Ser99, Asn100
5f	Asp163, π - cation- stacking- Arg95	Phe70, Tyr96, Pro37, Tyr39, Tyr165, Leu52, Tyr103	Asp9, Asp163, Glu166	Arg74, Arg95, Arg160	Ser99, Asn100
5g	Asn100, π - cation- stacking- Arg95	Tyr103, Phe36, Phe70, Pro37, Tyr39, Tyr165, Ala67	Asp9, Asp163, Glu166	Arg74, Arg95, Arg160	Ser99, Asn100, Ser104
5h	π -cation- stacking- Arg95	Phe70, Phe36, Pro37, Tyr39, Leu52, Tyr103, Tyr165	Asp9, Asp163, Glu166	Arg74, Arg95, Arg160	Ser99, Asn100
5i	Asp163, π - cation- stacking- Arg95	Pro37, Ala35, Tyr39, Phe36, Tyr165, Leu52, Phe70, Ala11	Asp9, Asp94, Asp163, Glu166	Arg14, Lys13, Arg153, Arg95, Arg160	-

5j	-	Phe70, Phe36, Pro37, Tyr39, Leu52, Tyr103, Tyr165	Asp9, Asp163, Glu166	Arg74, Arg95, Arg160	Ser99, Asn100
5k	Asn100, π - cation- stacking- Arg95	Tyr103, Phe70, Pro37, Tyr39, Tyr165, Ala67	Asp9, Asp163, Glu166	Arg74, Arg95, Arg160	Ser99, Asn100, Ser104, Gln172
5l	Asn100, π - cation- stacking- Arg95	Tyr103, Phe70, Pro37, Tyr39, Tyr165, Ala67	Asp9, Asp163, Glu166	Arg74, Arg95	Ser99, Asn100, Ser104
5m	Asn100	Tyr103, Phe70, Pro37, Tyr39, Tyr165, Ala67	Asp9, Asp163, Glu166	Arg74, Arg95	Ser99, Asn100, Ser104
5n	Arg95	Pro37, Phe70, Tyr96, Ala49, Tyr39, Leu52, Tyr103, Tyr165	Asp9, Asp163, Glu166	Arg74, Arg95, Lys13, Arg160	Ser99, Asn100, His53
5o	Asn100, π - cation- stacking- Arg95	Phe70, Phe36, Pro37, Tyr39, Leu52, Tyr103, Tyr16, Ala67	Asp9, Asp163, Glu166	Arg74, Arg95, Arg160	Ser99, Asn100, Ser104
5p	Lys13	Phe70, Tyr103, Tyr39, Pro37, Ala35, Ala49, Leu52, Tyr165	Asp9, Asp163, Asp94	Lys13, Arg95, Arg14, Arg160	Ser99, His53
5q	-	Phe70, Tyr96, Pro37, Phe36, Tyr39, Tyr103, Tyr165	Asp9, Asp163, Glu166	Arg74, Arg95, Arg160	Ser99, Asn100, Ser104
5r	Asn100, Tyr39, π - cation- stacking- Arg95	Tyr103, Phe36, Phe70, Pro37, Tyr39, Ala67, Tyr165	Asp9, Asp163, Glu166	Arg74, Arg95, Arg160	Ser99, Asn100, Ser104, Gln172
5s	Asn100, π -	Phe70, Phe36, Pro37,	Asp9,	Arg74,	Ser99,

	cation-stacking-Arg95	Tyr39, Tyr103, Ala67, Tyr165	Asp163, Glu166	Arg95, Arg160	Asn100, Ser104
5t	Asn100	Phe70, Pro37, Tyr165, Tyr103, Met66, Val63, Ala67	-	Arg74, Arg95, Arg107	Ser99, Asn100, Ser104

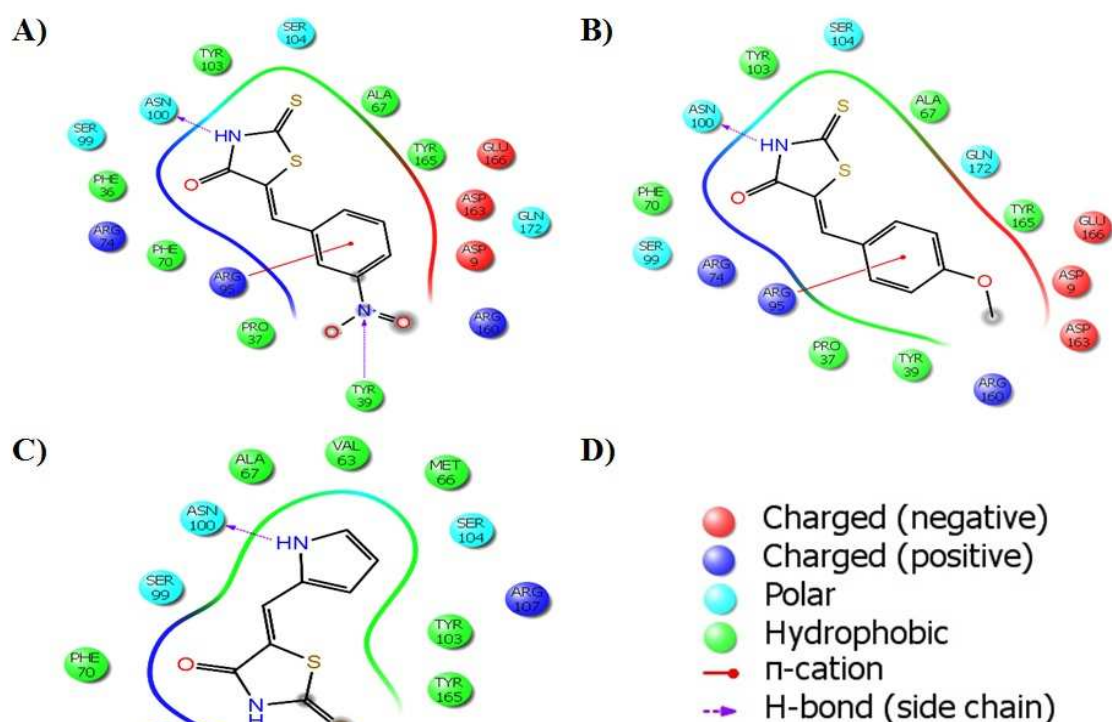


Figure 6: A) Ligand interaction diagram of compound **5r**. B) Ligand interaction diagram of compound **5k**. C) Ligand interaction diagram of compound **5t**. D) Ligand interaction diagram legend.

2.3.3 Molecular dynamic simulation

The obtained docking results allowed us to know a general and reasonable binding mode of the ligands and to ascertain the residues involved in the ligand recognition. Nevertheless, we decided to perform a molecular dynamic simulation of a ligand-receptor complex for further investigation of binding modes of ligand and to explicate the effects of ligand binding on the conformation of protein. Hence, the ligand **5k-1G3U** (5k-thymidylate kinase) complex (top-ranked docking

ligand-receptor complex) was selected as a representation for MD (Molecular Dynamic) simulation. The aim of MD simulation was to get more appropriate ligand-receptor model in a close state to the natural conditions and to further investigate the binding modes of the ligand, in the view of the fact that MD simulation can account for even the smaller variances.

The conformational stability of the **5k-1G3U** complex in the simulation procedure was assessed by carrying out a 50ns (nanoseconds) molecular dynamic simulation using Desmond (Schrodinger[®]) and analysed with Maestro's trajectory Visualizer. The trajectories were stable throughout the MD simulation run. The trajectory stability was checked and was substantiated by the analysis of protein-ligand RMSD (Root Mean Square Deviation) **Figure 7**.

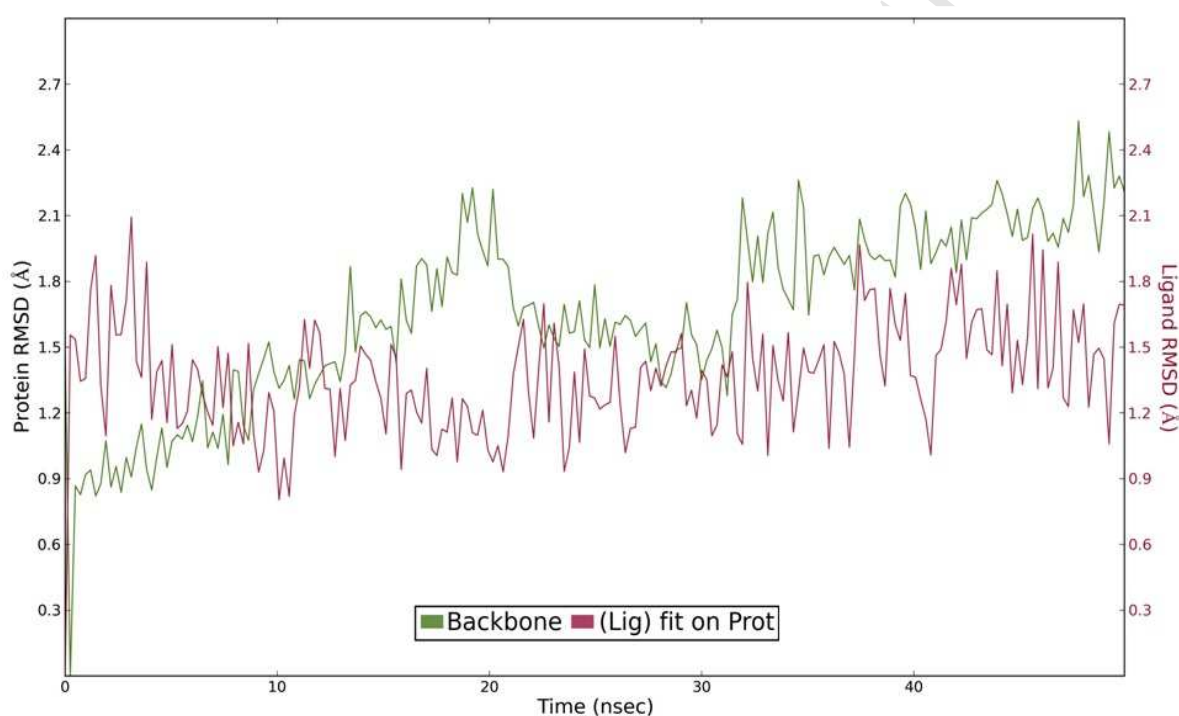


Figure 7: Plot showing Protein-Ligand RMSD evolution

Figure 7 reveals that the protein RMSD values (left Y-axis) have some acceptable fluctuations which did not exceed $\sim 2.5\text{\AA}$ throughout the MD simulation run. This indicates that the protein is stable without any notable conformational changes during the simulation run. In case of ligand RMSD (right Y-axis) the fluctuations did not exceed $\sim 2.1\text{\AA}$ throughout the MD simulation run. Moreover the observed ligand RMSD values are smaller than RMSD values of the protein, which indicates the stability of the ligand with respect to the protein and its binding pocket.

At the end of the MD simulation, position and orientation of ligand in the introduced binding site were changed (**Figure 8**) and this important observation indicates useful application of MD simulation after docking of ligands in the binding site. Explorative run of the MD simulation on the **5k-1G3U** complex revealed that except for Asn100, Arg95, Tyr165 and Phe70 the rest of

residues of the active site determined by docking were changed. The residues such as Tyr103 and Arg74 are newly positioned in proximity of ligand and participated in the interaction. At the end of MD simulation a new hydrogen bonding was found to exist between docked molecule and Arg74. Compound **5k** is also stabilized by an extra hydrophobic π - π -stacking interaction with Tyr103 which does not exist before MD simulation. On the other end, the hydrophobic interactions (Ala67, Pro37 and Tyr39) and electrostatic interactions (Arg160, Glu66, Asp9 and Asp163) with the ligand were vanished. Finally the difference in the orientation of ligand **5k** in binding modes after MD simulation was also noticed.

These results revealed that MD simulation obligate ligand to optimize its orientation and distance to binding site for maximum interaction with receptor. On docking of compound **5k** with 1G3U, the lowest energy confirmation did not show any hydrogen bonding and hydrophobic π - π -stacking interactions with amino acid residues Arg74 and Tyr103 respectively due to the absence of appropriate orientation and distance as was observed at the MD simulation. Ligand interaction pattern with percentage of contacts (interactions that occur more than 20.0% of the simulation time) of the ligand **5k** against 1G3U & BAR representation of the conserved binding site residues which influenced compound **5k** against 1G3U were shown in **Figure 8 & 9**.

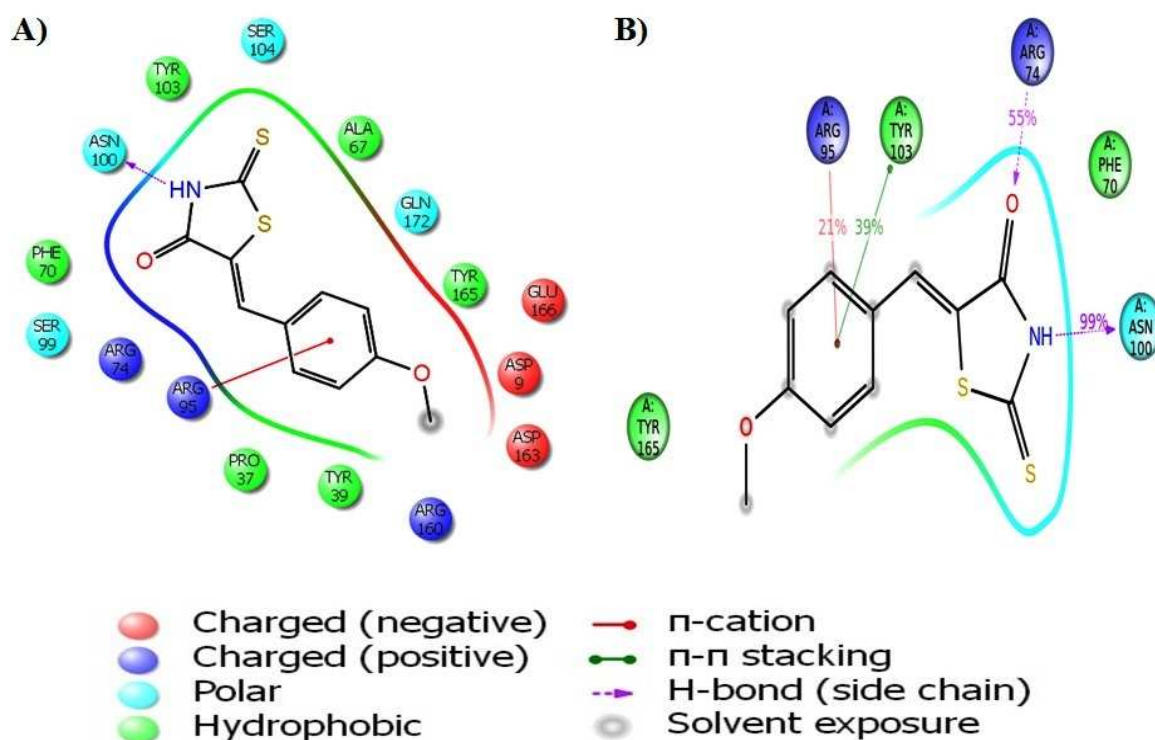


Figure 8: A) Ligand interaction pattern of the ligand **5k** against 1G3U before MD simulation. B) Ligand interaction pattern with percentage of contacts of the ligand **5k** against 1G3U after MD simulation.

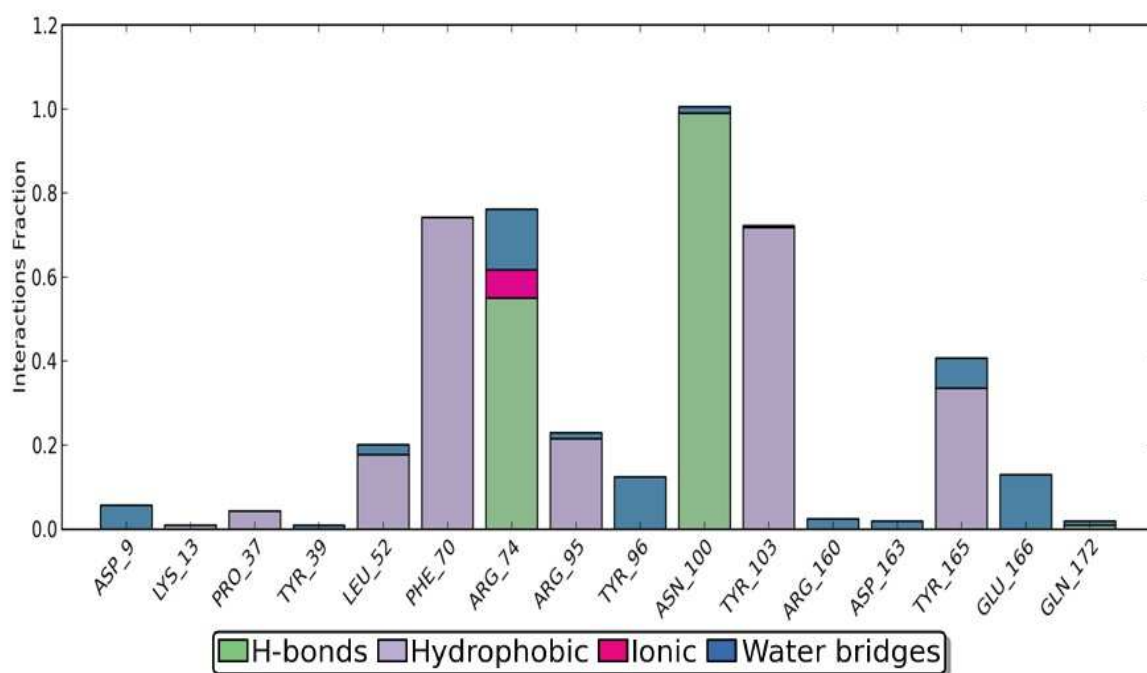


Figure 9: BAR representation of the conserved binding site residues which influenced compound **5k** against 1G3U.

3. Conclusion

In this work, the synthesis and *in-vitro* antimycobacterial activity evaluation and chemical features responsible for inhibitory activity of 2-thixo-1, 3-thiazolidine-4-one derivatives have been described. Compounds **5k**, **5r** and **5t** exhibited good *in-vitro* antimycobacterial activity at 0.05, 0.1, 0.2 $\mu\text{g/ml}$ concentrations respectively.

The results of Qikprop analysis gave information about the drug likeness properties of the compounds and all the compounds were found to be within the recommended values for 95% of known drugs. The molecular docking results and cross observational analysis suggested that the protein thymidylate kinase (**1G3U**) could be the plausible target for the tested compounds. The study also threw light about the various interaction patterns like hydrogen bonding, hydrophobic and electrostatic interactions between the ligands and the amino acid residues in the binding site. The docking results of ligands **5a-t** with **1G3U** protein gave information about the general binding mode and orientation of the ligands with respect to the receptor. In order to further investigate the binding modes of ligands on the confirmation of protein, **5k-1G3U** ligand-protein complex was selected as representative for the MD simulation study. The MD study suggested

the stability of both protein and ligand throughout the simulation time (50ns) as observed by the analysis of RMSD values of the both ligand and protein.

At the end of the MD simulation, the position and orientation of ligands introduced into the binding site were changed and this important observation indicates the useful application of MD simulation. Explorative run of MD simulation on the **5k-1G3U** complex revealed changes in some of the active site residues which were determined by docking. A new hydrogen bonding and an extra hydrophobic π - π stacking interaction was also noticed which did not exist before MD simulation. These results strongly suggests that MD simulation obligate the ligand to optimize its orientation and distance to the binding site for maximum interaction with receptor which was not observed in the docked complex before the MD simulation.

The tested compounds constitute an interesting lead for the evaluation of antimycobacterial activity. The optimized binding sites after MD simulation run can serve as a standard binding model.

4. Experimental

Melting points were taken using open capillary tubes and are uncorrected. ¹H, ¹³C NMR spectra were recorded on a Bruker 500 MHZ instrument in DMSO-d₆. Chemical shifts are given in parts per million. IR spectra were recorded on a Perkin-Elmer Spectrometer using KBr pellets. MASS Spectra were recorded on a Perkin Elmer Clarus 600 (EI) instrument. Elemental analyses were performed on a Perkin Elmer 2400 Series II Elemental CHNS analyzer. X-ray crystallographic study for one of the synthetic derivative was performed on a Bruker Kappa APEXII instrument.

4.1. Synthesis of 2-thioxo-1, 3-thiazolidin-4-ones 5

4.1.1. General procedure

A mixture of malononitrile (1.1 mmol) and substituted aldehydes (1.0 mmol) in ethanol in the presence of triethylamine was stirred at room temperature. After the complete disappearance of both starting materials (monitored by TLC), 2-thioxo-1, 3-thiazolidin-4-one(1.0 mmol) was added and the stirring was continued for 2 -2½hrs. The completion of the reaction was monitored by TLC. The solid formed in the reaction mixture was filtered, dried and recrystallized in ethanol to obtain the pure product in good yields.

4.1.1.1. (*Z*)-5-benzylidene-2-thioxothiazolidin-4-one (**5a**). Solid; (Yield 92%); mp 200-202°C; IR (KBr, ν_{\max}) cm^{-1} : 1488.94 (Ar C-C), 1674.09 (C=O), 1704.95 (C=S), 2923.87 (=C-H), 3062.73 (Ar C-H), 3463.90 (N-H); ^1H NMR (DMSO- D_6) δ : 7.49-7.56 (m, 3H, Ar-H), 7.60 (d, 2H, Ar-H), 7.65 (s, 1H, =CH-), 13.83 (s, 1H, N-H); ^{13}C NMR (DMSO- D_6) δ : 116.17, 126.00, 129.91, 130.93, 131.19, 132.10, 133.44, 143.11, 169.81, 196.16; MS (EI): m/z 221.05 [M^+]; Anal. Calcd. for $\text{C}_{10}\text{H}_7\text{NOS}_2$: C, 54.27; H, 3.19; N, 6.33; Found: C, 54.18; H, 3.18; N, 6.34.

4.1.1.2. (*Z*)-5-(4-chlorobenzylidene)-2-thioxothiazolidin-4-one (**5b**). Solid; (Yield 86%); mp 210-212 °C; IR (KBr, ν_{\max}) cm^{-1} : 825.47 (C-Cl), 1442.65 (Ar C-C), 1596.94 (C=O), 1704.95 (C=S), 2923.87 (=C-H), 3085.88 (Ar C-H), 3479.33 (N-H); ^1H NMR (DMSO- D_6) δ : 7.59-7.63 (m, 4H, Ar-H), 7.64 (s, 1H, =CH-), 13.88 (s, 1H, N-H); ^{13}C NMR (DMSO- D_6) δ : 115.14, 126.78, 129.98, 130.65, 132.36, 132.53, 135.82, 140.43, 169.78, 195.88; MS (EI): m/z 255.05 [M^+]; Anal. Calcd. for $\text{C}_{10}\text{H}_6\text{ClNOS}_2$: C, 46.96; H, 2.36; N, 5.48; Found: C, 46.85; H, 2.35; N, 5.49.

4.1.1.3. (*Z*)-5-(4-(dimethylamino)benzylidene)-2-thioxothiazolidin-4-one (**5c**). Solid; (Yield 95%); mp 272-274°C; IR (KBr, ν_{\max}) cm^{-1} : 1249.78 (amine C-N), 1442.65 (Ar C-C), 1612.37 (C=O), 1681.80 (C=S), 2854.44 (alkane C-H), 2916.16 (=C-H), 3039.59 (Ar C-H), 3457.06 (N-H); ^1H NMR (DMSO- D_6) δ : 3.03 (s, 3H, N- CH_3), 3.10 (s, 3H, N- CH_3), 6.81-6.85 (q, 2H, Ar-H), 7.41 (d, 1H, Ar-H), 7.51 (s, 1H, =CH-), 7.83 (d, 1H, Ar-H), 13.54 (s, 1H, N-H); ^{13}C NMR (DMSO- D_6) δ : 68.19, 69.15, 115.99, 117.83, 119.23, 120.26, 133.36, 133.73, 134.06, 152.25, 169.88, 195.47; MS (EI): m/z 264.16 [M^+]; Anal. Calcd. for $\text{C}_{12}\text{H}_{12}\text{N}_2\text{OS}_2$: C, 54.52; H, 4.58; N, 10.60; Found: C, 54.44; H, 4.59; N, 10.58.

4.1.1.4. (*Z*)-5-(4-(benzyloxy)benzylidene)-2-thioxothiazolidin-4-one (**5d**). Solid; (Yield 89%); mp 230-232 °C; IR (KBr, ν_{\max}) cm^{-1} : 1249.78 (ether C-O), 1442.65 (Ar C-C), 1589.23 (C=O), 1689.52 (C=S), 2854.44 (alkane C-H), 2923.87 (=C-H), 3055.02 (Ar C-H), 3456.18 (N-H); ^1H NMR (DMSO- D_6) δ : 5.22 (d, 2H, CH_2), 7.19 (d, 2H, Ar-H), 7.33-7.37 (q, 1H, Ar-H), 7.41 (t, 2H, Ar-H), 7.47 (d, 2H, Ar-H), 7.57 (d, 2H, Ar-H), 7.61 (s, 1H, =CH-), 13.74 (s, 1H, NH); ^{13}C NMR (DMSO- D_6) δ : 70.04, 115.26, 126.16, 128.28, 128.43, 128.51, 128.66, 128.97, 129.01, 132.27, 133.14, 133.82, 136.51, 136.91, 141.24, 160.90, 163.89, 169.92, 195.98; MS (EI): m/z 327.17 [M^+]; Anal. Calcd. for $\text{C}_{17}\text{H}_{13}\text{NO}_2\text{S}_2$: C, 62.36; H, 4.00; N, 4.28; Found: C, 62.20; H, 4.01; N, 4.27.

4.1.1.5. (Z)-5-(4-hydroxy-3-methoxybenzylidene)-2-thioxothiazolidin-4-one (**5e**). Solid; (Yield 90%); mp220-222°C; IR (KBr, ν_{\max}) cm^{-1} : 1280.64 (alcoholic C-O), 1442.65 (Ar C-C), 1589.23 (C=O), 1712.66 (C=S), 2854.44 (alkane C-H), 2923.87 (=C-H), 3008.73 (Ar C-H), 3340.46 (N-H), 3610.48 (O-H); ^1H NMR (DMSO- D_6) δ : 3.82 (s, 3H, O- CH_3), 6.93 (d, 1H, Ar-H), 7.06 (d, 1H, Ar-H), 7.11 (s, 1H, Ar-H), 7.54 (s, 1H, =CH-), 10.13 (s, 1H, Ar-OH), 13.62 (s, 1H, N-H); ^{13}C NMR (DMSO- D_6) δ : 56.11, 114.73, 121.06, 124.86, 125.55, 133.25, 134.90, 137.44, 148.59, 169.88, 195.90; MS (EI): m/z 267.15 [M^+]; Anal. Calcd. for $\text{C}_{11}\text{H}_9\text{NO}_3\text{S}_2$: C, 49.42; H, 3.39; N, 5.24; Found: C, 49.29; H, 3.38; N, 5.23.

4.1.1.6. (Z)-5-(2-hydroxybenzylidene)-2-thioxothiazolidin-4-one (**5f**). Solid; (Yield 88%); mp158-160°C; IR (KBr, ν_{\max}) cm^{-1} : 1280.64 (alcoholic C-O), 1442.65 (Ar C-C), 1653.52 (C=O), 1743.52 (C=S), 2862.15 (=C-H), 3116.74 (Ar C-H), 3340.46 (N-H), 3633.62 (O-H); ^1H NMR (DMSO- D_6) δ : 5.03 (s, 1H, O-H), 7.02-7.04 (q, 1H, Ar-H), 7.17-7.22 (m, 2H, Ar-H), 7.30-7.34 (m, 1H, Ar-H), 7.44 (d, 1H, =CH-), 13.32 (s, 1H, N-H); ^{13}C NMR (DMSO- D_6) δ : 116.65, 120.22, 120.81, 125.54, 128.92, 129.77, 130.89, 149.68, 176.34, 203.70; MS (EI): m/z 237.26 [M^+]; Anal. Calcd. for $\text{C}_{10}\text{H}_7\text{NO}_2\text{S}_2$: C, 50.61; H, 2.97; N, 5.90; Found: C, 50.77; H, 2.96; N, 5.91.

4.1.1.7. (Z)-5-(4-nitrobenzylidene)-2-thioxothiazolidin-4-one (**5g**). Solid; (Yield 85%); mp240-242 °C; IR (KBr, ν_{\max}) cm^{-1} : 1342.36 (nitro N-O), 1411.79 (Ar C-C), 1604.66 (C=O), 1720.38 (C=S), 2923.87 (=C-H), 3016.45 (Ar C-H), 3440.76 (N-H); ^1H NMR (DMSO- D_6) δ : 7.73 (s, 1H, =CH-), 7.86 (t, 2H, Ar-H), 8.32-8.34 (m, 2H, Ar-H), 14.00 (s, 1H, NH); ^{13}C NMR (DMSO- D_6) δ : 116.96, 124.79, 129.03, 130.44, 131.76, 135.33, 139.67, 147.99, 169.70, 195.73; MS (EI): m/z 266.11 [M^+]; Anal. Calcd. for $\text{C}_{10}\text{H}_6\text{N}_2\text{O}_3\text{S}_2$: C, 45.10; H, 2.27; N, 10.52; Found: C, 45.31; H, 2.26; N, 10.55.

4.1.1.8. (Z)-5-(2-bromobenzylidene)-2-thioxothiazolidin-4-one(**5h**). Solid; (Yield 92%); mp236-238 °C; IR (KBr, ν_{\max}) cm^{-1} : 604.87 (C-Br), 1450.36 (Ar C-C), 1604.66 (C=O), 1728.09 (C=S), 2923.87 (=C-H), 3109.02 (Ar C-H), 3440.76 (N-H); ^1H NMR (DMSO- D_6) δ : 7.40-7.45 (m, 1H, Ar-H), 7.51-7.59 (m, 2H, Ar-H), 7.72 (s, 1H, =C-H), 7.81 (t, 1H, Ar-H), 13.96 (s, 1H, N-H); ^{13}C NMR (DMSO- D_6) δ : 117.18, 128.86, 129.11, 129.40, 132.21, 132.54, 133.71, 142.54, 169.05, 195.58; MS (EI): m/z 300.01 [M^+]; Anal. Calcd. for $\text{C}_{10}\text{H}_6\text{BrNOS}_2$: C, 40.01; H, 2.01; N, 4.67; Found: C, 40.19; H, 2.00; N, 4.68.

4.1.1.9. (Z)-5-(2,3-difluoro-6-methoxybenzylidene)-2-thioxothiazolidin-4-one (**5i**). Solid; (Yield 93%); mp188-190°C; IR (KBr, ν_{\max}) cm^{-1} : 1080.06 (C-F), 1203.49 (ether C-O), 1434.93 (Ar C-C), 1581.51 (C=O), 1697.23 (C=S), 2854.44 (alkane C-H), 3109.02 (=C-H), 3147.60 (Ar C-H), 3556.48 (N-H); ^1H NMR (DMSO- D_6) δ : 3.91 (s, 3H, O- CH_3), 6.95-6.98 (m, 1H, Ar-H), 7.51 (s, 1H, =CH-), 7.54-7.62 (q, 1H, Ar-H), 13.78 (s, 1H, N-H); ^{13}C NMR (DMSO- D_6) δ : 56.20, 111.46, 119.83, 120.01, 120.20, 120.25, 120.28, 130.44, 142.92, 169.07, 196.44; MS (EI): m/z 287.18 [M^+]; Anal. Calcd. for $\text{C}_{11}\text{H}_7\text{F}_2\text{NO}_2\text{S}_2$: C, 45.99; H, 2.46; N, 4.88; Found: C, 45.75; H, 2.45; N, 4.89.

4.1.1.10. (Z)-5-((benzo[*b*]thiophen-3-yl)methylene)-2-thioxothiazolidin-4-one(**5j**). Solid; (Yield 88%); mp244-246 °C;IR (KBr, ν_{\max}) cm^{-1} : 1427.22 (Ar C-C), 1589.23 (C=O), 1697.23 (C=S), 2839.01 (=C-H), 3062.73 (Ar C-H), 3456.18 (N-H); ^1H NMR (DMSO- D_6) δ : 7.50-7.55 (m, 2H, Ar-H), 7.88 (s, 1H, =CH-), 8.09-8.16 (m, 3H, Ar-H), 13.87 (s, 1H, N-H); ^{13}C NMR (DMSO- D_6) δ : 114.01, 125.34, 125.64, 125.71, 125.94, 126.65, 127.74, 138.72, 139.12, 151.00, 169.08, 195.38; MS (EI): m/z 277.14 [M^+]; Anal. Calcd. for $\text{C}_{12}\text{H}_7\text{NOS}_3$: C, 51.96; H, 2.54; N, 5.05; Found: C, 52.11; H, 2.53; N, 5.04.

4.1.1.11. (Z)-5-(4-methoxybenzylidene)-2-thioxothiazolidin-4-one(**5k**). Solid; (Yield 87%); mp280-282 °C;IR (KBr, ν_{\max}) cm^{-1} : 1257.50 (ether C-O), 1442.65 (Ar C-C), 1689.52 (C=O), 1751.24 (C=S), 2923.87 (alkane C-H), 3008.73 (=C-H), 3132.17 (Ar C-H), 3471.61 (N-H); ^1H NMR (DMSO- D_6) δ : 3.84 (s, 3H, O- CH_3), 7.10 (d, 2H, Ar-H), 7.56 (d, 2H, Ar-H), 7.60 (s, 1H, =CH-), 13.74 (s, 1H, NH); ^{13}C NMR (DMSO- D_6) δ : 55.53, 115.06, 122.19, 125.45, 128.05, 131.86, 132.66, 133.59, 144.24, 169.39, 195.47; MS (EI): m/z 251.25 [M^+]; Anal. Calcd. for $\text{C}_{11}\text{H}_9\text{NO}_2\text{S}_2$: C, 52.57; H, 3.61; N, 5.57; Found: C, 52.39; H, 3.62; N, 5.56.

4.1.1.12. (Z)-5-((furan-2-yl)methylene)-2-thioxothiazolidin-4-one (**5l**). Solid; (Yield 85%); mp225-227 °C;IR (KBr, ν_{\max}) cm^{-1} : 1442.65 (Ar C-C), 1689.52 (C=O), 1797.52 (C=S), 2923.87 (=C-H), 3031.88 (Ar C-H), 3456.18 (N-H); ^1H NMR (DMSO- D_6) δ : 6.76-6.78 (q, 1H, hetero Ar-H), 7.18 (d, 1H, hetero Ar-H), 7.49 (s, 1H, =CH-), 8.11 (d, 1H, hetero Ar-H), 13.69 (s, 1H, NH); ^{13}C NMR (DMSO- D_6) δ : 113.89, 119.85, 122.42, 129.54, 135.72, 148.29, 168.98, 196.47; MS (EI): m/z 211.20 [M^+]; Anal. Calcd. for $\text{C}_8\text{H}_5\text{NO}_2\text{S}_2$: C, 45.48; H, 2.39; N, 6.63; Found: C, 45.39; H, 2.38; N, 6.64.

4.1.1.13. (Z)-5-((thiophen-2-yl)methylene)-2-thioxothiazolidin-4-one (**5m**). Solid; (Yield 92%); mp252-254 °C; IR (KBr, ν_{\max}) cm^{-1} : 1434.93 (Ar C-C), 1681.80 (C=O), 1797.52 (C=S), 3078.16 (=C-H), 3139.88 (Ar C-H), 3556.48 (N-H); ^1H NMR (DMSO- D_6) δ : 7.29-7.32 (q, 1H, hetero Ar-H), 7.71 (d, 1H, hetero Ar-H), 7.92 (s, 1H, =CH-), 8.08 (d, 1H, hetero Ar-H), 13.79 (s, 1H, NH); ^{13}C NMR (DMSO- D_6) δ : 122.96, 124.77, 129.27, 134.30, 135.38, 137.42, 169.00, 194.59; MS (EI): m/z 227.10 [M^+]; Anal. Calcd. for $\text{C}_8\text{H}_5\text{NOS}_3$: C, 42.27; H, 2.22; N, 6.16; Found: C, 42.49; H, 2.21; N, 6.17.

4.1.1.14. (Z)-5-(3,4,5-trimethoxybenzylidene)-2-thioxothiazolidin-4-one(**5n**). Solid; (Yield 84%); mp168-170°C; IR (KBr, ν_{\max}) cm^{-1} : 1249.78 (ether C-O), 1496.65 (Ar C-C), 1689.52 (C=O), 1766.67 (C=S), 2839.01 (alkane C-H), 2939.30 (=C-H), 3008.73 (Ar C-H), 3471.61 (N-H); ^1H NMR (DMSO- D_6) δ : 3.74 (s, 3H, O- CH_3), 3.83 (d, 6H, O- CH_3), 6.88 (s, 2H, Ar-H), 7.58 (s, 1H, =CH-), 13.82 (s, 1H, N-H); ^{13}C NMR (DMSO- D_6) δ : 55.98, 60.19, 60.42, 114.37, 124.23, 126.34, 128.39, 132.01, 139.74, 142.91, 153.23, 169.23, 195.42; MS (EI): m/z 311.10 [M^+]; Anal. Calcd. for $\text{C}_{13}\text{H}_{13}\text{NO}_4\text{S}_2$: C, 50.14; H, 4.21; N, 4.50; Found: C, 49.98; H, 4.22; N, 4.49.

4.1.1.15. (Z)-5-((naphthalen-2-yl)methylene)-2-thioxothiazolidin-4-one (**5o**). Solid; (Yield 89%); mp290-292 °C; IR (KBr, ν_{\max}) cm^{-1} : 1427.22 (Ar C-C), 1704.95 (C=O), 1789.81 (C=S), 2923.87 (=C-H), 3070.45 (Ar C-H), 3448.47 (N-H); ^1H NMR (DMSO- D_6) δ : 7.60-7.69 (m, 3H, Ar-H), 7.79 (s, 1H, =CH-), 7.98 (t, 1H, Ar-H), 8.06 (t, 2H, Ar-H), 8.19 (s, 1H, Ar-H), 13.88 (s, 1H, N-H); ^{13}C NMR (DMSO- D_6) δ : 116.12, 127.20, 127.71, 128.21, 128.84, 129.08, 129.56, 130.55, 131.49, 131.60, 132.76, 140.62, 169.45, 195.73; MS (EI): m/z 271.12 [M^+]; Anal. Calcd. for $\text{C}_{14}\text{H}_9\text{NOS}_2$: C, 61.97; H, 3.34; N, 5.16; Found: C, 61.79; H, 3.35; N, 5.15.

4.1.1.16. (Z)-5-((anthracen-9-yl)methylene)-2-thioxothiazolidin-4-one (**5p**). Solid; (Yield 90%); mp218-220 °C; IR (KBr, ν_{\max}) cm^{-1} : 1442.65 (Ar C-C), 1620.09 (C=O), 1743.52 (C=S), 3016.45 (=C-H), 3055.02 (Ar C-H), 3448.47 (N-H); ^1H NMR (DMSO- D_6) δ : 7.62-7.72 (m, 4H, Ar-H), 8.16-8.22 (q, 4H, Ar-H), 8.88 (s, 1H, =CH-), 9.66 (s, 1H, Ar-H); ^{13}C NMR (DMSO- D_6) δ : 113.88, 123.97, 125.05, 125.36, 126.33, 126.55, 128.34, 128.89, 129.56, 129.77, 129.84, 130.93, 131.90, 139.48, 163.07, 195.82; MS (EI): m/z 321.23 [M^+]; Anal. Calcd. for $\text{C}_{18}\text{H}_{11}\text{NOS}_2$: C, 67.26; H, 3.45; N, 4.36; Found: C, 67.01; H, 3.44; N, 4.37.

4.1.1.17. (Z)-5-(2-nitrobenzylidene)-2-thioxothiazolidin-4-one (**5q**). Solid; (Yield 85%); mp250-252 °C; IR (KBr, ν_{\max}) cm^{-1} : 1458.08 (Ar C-C), 1527.51 (nitro N-O), 1697.23 (C=O), 1735.81 (C=S), 2923.87 (=C-H), 3093.59 (Ar C-H), 3409.90 (N-H); ^1H NMR (DMSO- D_6) δ : 7.70-7.76 (m, 2H, Ar-H), 7.87-7.91 (q, 2H, Ar-H), 8.20-8.22 (q, 1H, =CH-), 13.96 (s, 1H, N-H); ^{13}C NMR (DMSO- D_6) δ : 117.18, 127.80, 128.72, 129.36, 130.31, 131.21, 134.56, 147.92, 168.60, 195.73; MS (EI): m/z 266.04 [M^+]; Anal. Calcd. for $\text{C}_{10}\text{H}_6\text{N}_2\text{O}_3\text{S}_2$: C, 45.10; H, 2.27; N, 10.52; Found: C, 45.29; H, 2.26; N, 10.51.

4.1.1.18. (Z)-5-(3-nitrobenzylidene)-2-thioxothiazolidin-4-one (**5r**). Solid; (Yield 94%); mp236-238 °C; IR (KBr, ν_{\max}) cm^{-1} : 1419.50 (Ar C-C), 1527.51 (nitro N-O), 1697.23 (C=O), 1797.52 (C=S), 3008.73 (=C-H), 3093.59 (Ar C-H), 3348.18 (N-H); ^1H NMR (DMSO- D_6) δ : 7.76 (s, 1H, =CH-), 7.82 (t, 1H, Ar-H), 8.00 (d, 1H, Ar-H), 8.28-8.30 (q, 1H, Ar-H), 8.43 (t, 1H, Ar-H), 13.96 (br-s, 1H, N-H); ^{13}C NMR (DMSO- D_6) δ : 120.38, 124.47, 124.64, 128.37, 129.23, 130.94, 134.80, 135.68, 170.13, 195.58; MS (EI): m/z 266.11 [M^+]; Anal. Calcd. for $\text{C}_{10}\text{H}_6\text{N}_2\text{O}_3\text{S}_2$: C, 45.10; H, 2.27; N, 10.52; Found: C, 44.98; H, 2.28; N, 10.53.

4.1.1.19. (Z)-5-((1H-indol-3-yl)methylene)-2-thioxothiazolidin-4-one (**5s**). Solid; (Yield 86%); mp248-250 °C; IR (KBr, ν_{\max}) cm^{-1} : 1434.93 (Ar C-C), 1566.08 (C=O), 1681.80 (C=S), 3039.59 (=C-H), 3116.74 (Ar C-H), 3456.18 (N-H); ^1H NMR (DMSO- D_6) δ : 7.20-7.29 (m, 2H, Ar-H), 7.51 (d, 1H, =CH-), 7.83 (d, 1H, hetero Ar-H), 7.93 (d, 2H, Ar-H), 12.31 (s, 1H, indole N-H), 13.56 (s, 1H, N-H); ^{13}C NMR (DMSO- D_6) δ : 112.50, 117.86, 118.44, 121.37, 123.25, 124.76, 126.74, 130.01, 136.37, 140.20, 169.10, 194.61; MS (EI): m/z 260.20 [M^+]; Anal. Calcd. for $\text{C}_{12}\text{H}_8\text{N}_2\text{OS}_2$: C, 55.36; H, 3.10; N, 10.76; Found: C, 55.21; H, 3.11; N, 10.75.

4.1.1.20. (Z)-5-((1H-pyrrol-2-yl)methylene)-2-thioxothiazolidin-4-one (**5t**). Solid; (Yield 88%); mp245-247 °C; IR (KBr, ν_{\max}) cm^{-1} : 1442.65 (Ar C-C), 1596.94 (C=O), 1704.95 (C=S), 2923.87(=C-H), 3085.88 (Ar C-H), 3479.33 (N-H); ^1H NMR (DMSO- D_6) δ : 6.39-6.41 (q, 1H, Hetero Ar-H), 6.53 (s, 1H, hetero Ar-H), 7.27-7.29 (m, 1H, hetero Ar-H), 7.52 (s, 1H, =CH-), 11.80 (s, 1H, pyrrole NH), 13.53 (s, 1H, NH); ^{13}C NMR (DMSO- D_6) δ : 114.97, 121.94, 125.71, 127.21, 132.95, 139.34, 169.18, 194.77; MS (EI): m/z 210.12 [M^+]; Anal. Calcd. for $\text{C}_8\text{H}_6\text{N}_2\text{OS}_2$: C, 45.69; H, 2.88; N, 13.32; Found: C, 45.58; H, 2.89; N, 13.31.

4.2. *In-vitro* antimycobacterial activity

Briefly, 200 μ L of sterile deionized water was added to all outer perimeter wells of sterile 96 well plates to minimize evaporation of the medium in the test wells during incubation. The 96 plates received 100 μ L of the Middlebrook 7H9 broth and a serial dilution of the compounds were made directly on the plate. The final drug concentrations tested were 100.0-0.003 μ g/mL. Plates were covered and sealed with parafilm and were incubated at 37 °C for 5 days. After this time, 25 μ L of a freshly prepared 1:1 mixture of Alamar Blue (Accumed International, Westlake Ohio) reagent and 10% Tween 80 were added to the plate and was incubated for 24 h. A blue color in the well was interpreted as no bacterial growth, and a pink color was scored as growth. The MIC (Minimal Inhibition Concentration) was defined as the lowest drug concentration, which prevented a color change from blue to pink. The test has been performed in triplicate.

4.3. Computational studies

The computational studies were performed by performed by maestro 9.3 (Maestro[®]v-9.3.515 (Schrodinger, LLC, New York, NY), running on Intel Core i5 3230M with Radeon(tm) HD Graphics 1.90 GHz, RAM Memory 4GB under Windows 8 system. The *In-silico* ADME properties, molecular docking and molecular dynamics studies were performed using QikProp, Glide and Desmond modules with default parameter settings.

Acknowledgements

One of the authors, KMN thanks Dr. Kishore Bhat, Director, Department of Molecular Biology and Immunology, Maratha Mandal's NGH Institute of Dental Sciences & Research Centre, Belgaum, Karnataka, for providing necessary facilities in studying *in-vitro* antimycobacterial assay. Abounded thanks are due to Dr. Raghu for providing the Schrodinger software and also for the encouragement and motivation to complete the computational studies. The author KMN thanks SIF-School of Advanced Sciences, VIT University, Vellore for providing the spectral data.

References:

1. V. Kumar, A.K. Abbas, N. Fausto, R.N. Mitchell, *Robbins Basic Pathology*. Saunders Elsevier. 8thed (2007) 516–522.
2. A. Konstantinos, Testing for tuberculosis. *Australian Prescriber* 33 (1) (2010)12–18.

3. "Tuberculosis Fact sheet N°104". World Health Organization. November (2010) Retrieved 26 July 2011.
4. "Tuberculosis". World Health Organization. (2002).
5. World Health Organization "Epidemiology". Global tuberculosis control: epidemiology, strategy and financing. (2009) 6–33.
6. "Improved data reveals higher global burden of tuberculosis". WHO.int. 22 October (2014) Retrieved 23 October 2014.
7. GBD 2013 Mortality and Causes of Death Collaborators., "Global, regional and national age-sex specific all-cause and cause-specific mortality for 240 causes of death, 1990-2013: a systematic analysis for the Global Burden of Disease Study 2013". *Lancet*. 385 (9963) (2014)117–171.
8. World Health Organization., "The sixteenth global report on tuberculosis-2011".
9. P.R. Mohapatra, *Am J Respir Crit Care Med*. 170(8) (2004) 920-1.
10. H.L. Rieder,*Lancet*. 373(9670) (2009) 1148-9.
11. G. Capan, et al., *Monatshefte für Chemie / Chemical Monthly*. 130(11) (1999) 1399-1407.
12. C.V. Kavitha, et al., *Bioorg Med Chem*. 14(7) (2006) 2290-99.
13. K. Omar, A. Geronikaki, P. Zoumpoulakis, C. Camoutsis, M. Sokovic, A. Ciric, J. Glamoclija, *Bioorg. Med. Chem. Lett*. 18 (2010) 426-32.
14. M.G. Vigorita, et al., *Bioorg Med Chem Lett*. 11(21) (2001) 2791-4.
15. R. Ottana, et al., *Bioorg Med Chem*. 13(13) (2005) 4243-52.
16. C.S. Kumar, S.K. Rajput, Bhati, *Bioorg. Med. Chem. Lett*. 15 (2007) 3089-96.
17. P. Karegoudar, et al., *Eur J Med Chem*. 43(4) (2008) 808-15.
18. R. Ottana, S. Carotti, R. Maccari, I. Landini, G. Chiricosta, B. Caciagli, M.G. Vigorita, E. Mini, *Bioorg. Med. Chem. Lett*. 15 (2005) 3930-3933.

19. A. Rao, A. Carbone, E. Chimirri, A.M. De Clercq, P. Monforte, C. Monforte, M.Z. Pannecouque, *Farmaco*. 58 (2003) 115-120.
20. M.L. Barreca, A. Chimirri, E. De Clercq, L. De Luca, A.M. Monforte, P. Monforte, A. Rao, M. Zappala, *Farmaco*. 58 (2003) 259-63.
21. G. Kucukguzel, et al., *Eur J Med Chem*. 41(3) (2006) 353-9.
22. R.K. Rawal, R. Tripathi, S.B. Katti, C. Pannecouque, E. De Clercq, *Bioorg. Med. Chem.* 15 (2007) 1725-31.
23. S. Karakus and S. Rollas, *Farmaco*. 57(7) (2002) 577-81.
24. K. Babaoglu, M.A. Page, V.C. Jones, M.R. McNeil, C. Dong, J.H. Naismith, R.E. Lee, *Bioorg. Med. Chem. Lett.* 13 (2003) 3227-30.
25. V.V. Kachhadia, M.R. Patel, H.S. Joshi, *J. Serb. Chem. Soc.* 70 (2005) 153.
26. A. Foroumadi, et al., *Bioorg Med Chem Lett.* 16(5) (2006) 1164-7.
27. L.A. Collins, G.F. Scott, *Antimicrobial Agents and Chemotherapy*. 41(5) (1997) 1004-1009.
28. J. L. Gershell, J.H. Atkins, *Nat Rev Drug Discovery*. 2 (2003) 321-27.
29. Karthik, R.; Kalidas, Y.; Nagasuma, C., *BMC Systems Biology*.2 (2008) 109.
30. K. Gokulan, B. Rupp, M.S. Pavelka, W.R. Jacob, J.C. Sacchettini, *J Biol Chem*. 278 (20) (2003) 18588-96.
31. C.C. Huang, V.S. Clare, M.S. Glickman, W.R. Jacob, J.C. Sacchettini, *J Biol Chem*. 277(13) (2002) 11559-69.
32. L.C. Graeme, A.P. Neil, A.S. Clyde, R. Bernhard, M.S. Brian, N.B. Edward, *J Biol Chem*. 280 (14) (2005) 13978-86.
33. C.E. Lee, C. Goodfellow, J.M. Farah, N.B. Edward, J.S. Lott, *J Mol Biol*. 355 (2006)784-797.

34. P. Sampathkumar, S. Turley, J.E. Ulmer, H.G. Rhie, C.H. Sibley, W.G. Hol, *J Mol Biol.* 352 (5) (2003) 1091-104.
35. H. Xin, A. Akram, R. Paul, O. Montellano, *Bioorg Med Chem.* 15 (2007) 6649–58.
36. S. Li de la, L.H. Munier, A.M. Gilles, O. Barzu, M. Delarue, *J Mol Biol.* 311 (2001) 87-100.
37. N. Scherr, S. Honnappa, G. Kunz, P. Mueller, R. Jayachandran, F. Winkler, J. Pieters, M.O. Steinmetz, *PNAS.* 104 (29) (2007) 12151-56.
38. E.M. Tretter, A.M. Berger, *J Biol Chem.* 287 (22) (2012) 18645-54.
39. S.B. Erdemli, R. Gupta, W.R. Bishai, G. Lamichhane, M. Amzel, M.A. Bianchet, *Structure.* 20 (12) (2012) 2103-115.